

Strongly coupled radiation from moving mirrors and holography in the Karch-Randall model

Oriol Pujolàs

*Center for Cosmology and Particle Physics,
Department of Physics, New York University,
New York, NY 10003, U.S.A.
E-mail: pujolas@ccpp.nyu.edu*

ABSTRACT: Motivated by the puzzles in understanding how Black Holes evaporate into a strongly coupled Conformal Field Theory, we study particle creation by an accelerating mirror. We model the mirror as a gravitating Domain Wall and consider a CFT coupled to it through gravity, in asymptotically Anti de Sitter space. This problem (backreaction included) can be solved exactly at one loop. At strong coupling, this is dual to a Domain Wall localized on the brane in the Karch-Randall model, which can be fully solved as well. Hence, in this case one can see how the particle production is affected by A) strong coupling and B) its own backreaction. We find that A) the amount of CFT radiation at strong coupling is not suppressed relative to the weak coupling result; and B) once the boundary conditions in the AdS_5 bulk are appropriately mapped to the conditions for the CFT on the boundary of AdS_4 , the Karch-Randall model and the CFT side agree to leading order in the backreaction. This agreement holds even for a new class of self-consistent solutions (the ‘Bootstrap’ Domain Wall spacetimes) that have no classical limit. This provides a quite precise check of the holographic interpretation of the Karch-Randall model. We also comment on the massive gravity interpretation.

As a byproduct, we show that relativistic Cosmic Strings (pure tension codimension 2 branes) in Anti de Sitter are repulsive and generate long-range tidal forces even at classical level. This is the phenomenon dual to particle production by Domain Walls.

KEYWORDS: Gauge-gravity correspondence, AdS-CFT Correspondence, Nonperturbative Effects, Black Holes.

Contents

1.	Introduction	1
2.	CFT radiation from Domain Walls	5
2.1	Preamble: Domain Walls as accelerating mirrors	5
2.2	Quantum conformal fields on DW backgrounds	7
2.2.1	Boundary conditions	9
2.2.2	Casimir energy on $AdS_3 \times S_1$ at weak coupling	13
2.3	Including the backreaction	15
2.3.1	Massive gravity interpretation	17
2.3.2	Bootstrap Domain Wall spacetimes	20
3.	5D gravity dual	23
3.1	Ignoring the backreaction (the brane)	24
3.1.1	Casimir energy on $AdS_3 \times S_1$ at strong coupling	24
3.2	Localized Domain Walls in the Karch-Randall model	26
4.	Epilogue: cosmic strings in AdS	30
5.	Conclusions	34

1. Introduction

The AdS/CFT correspondence [1–3] provides a powerful method to investigate the dynamics of strongly coupled gauge theories. The correspondence relates a supergravity theory around 5 dimensional Anti de Sitter space (AdS_5) with a Conformal Field Theory (CFT) defined on the boundary of AdS_5 and decoupled from gravity — in the limit of large number of colours N with the 't Hooft coupling $\lambda \equiv g_{\text{YM}}^2 N \gg 1$ fixed.

Dynamical gravity can be included in the 4D theory by breaking explicitly conformal invariance in the UV, which corresponds to the introduction of a brane in the AdS_5 bulk [4–6], that is, to the Randall Sundrum (RS) model [7]. This leads to a ‘cutoff’ version of the correspondence that can be sharply stated as relating the (classical) 5D solutions of the RS model with matter localized on the brane to 4D geometries where the quantum effects from the CFT and their backreaction are taken into account [8, 9]. If true, this extended version of the correspondence represents an almost tailor-made tool to study semiclassical gravity problems with strongly self-interacting fields.

In particular, this has led to a number of interesting claims concerning how Black Hole (BH) evaporation is affected by the strongly coupled nature of the field theory. Ignoring

the self-interactions (that is, for $\lambda = 0$), one expects the Hawking radiation to scale as N^2 . Since the backreaction from this flux of energy is automatically accounted for in the braneworld construction, one would conclude that there should be no static (large) BHs localized on a RS brane [9, 8]. However, as argued in [10] the strongly coupled nature of the CFT might render this conclusion invalid. If the CFT is in a confining phase, then the BH should actually emit colour singlet states, implying that there should be no N^2 enhancement in the radiation. Given that the 5D gravity dual gives the leading order contribution in the $1/N$ expansion, this would lead to zero Hawking radiation at this order. This is supported [10] by the (warped) uniform Black String (BS) solution [11] in the two-brane RS model [12]. This solution is stable for a large enough horizon radius, and displays no Hawking radiation from the 4D point of view. However, the dual of the two-brane RS model is a ‘CFT’ where conformal invariance is broken in the IR even in flat space (one is not really dealing with a massless theory), so it still seems unclear what happens for an unbroken CFT, that is, in the one-brane RS model (see also [13–17]).

A sharper situation arises for asymptotically AdS_4 Black Holes. The presence of a negative cosmological constant Λ_4 effectively places the system in a box, and the CFT can reach an equilibrium configuration with the BH. In this way one can avoid the technical problems associated with a putative time dependence of the asymptotically flat case. The correspondence in the presence of $\Lambda_4 < 0$ is perhaps not as well understood as for $\Lambda_4 = 0$, but the picture is that 4D gravity with $\Lambda_4 < 0$ and the strongly coupled CFT is dual to the Karch-Randall (KR) model [18] with either one or two branes, depending on the boundary conditions for the CFT fields at the AdS_4 boundary. The one-brane model arises with the so-called Karch-Randall boundary conditions (see below) [19–24]. Instead, with reflecting boundary conditions, one obtains a two-brane model with an additional Z_2 symmetry across the bulk. As shown in [25] (see also [26]), with reflecting boundary conditions the vacuum polarization at strong coupling dramatically differs from the weak coupling result. Indeed, for large enough horizon radii the uniform Black String solution is stable [27, 28], so this should be the physical solution. Clearly, this solution corresponds to a state of the CFT where the thermal component of $\langle T_{\mu\nu} \rangle^{\text{CFT}}$ vanishes. Since the one loop estimate is instead of order N^2 [25], one concludes that the ‘shutdown’ of the Hawking radiation must be a strong coupling effect. It is worth pointing out that even though the Schwarzschild- AdS_4 Black String is stable for the one-brane KR model as well, this solution does not seem relevant because the bulk is asymptotically substantially different from AdS_5 . Hence, with KR boundary conditions (i.e., again, in the one-brane case) we do not expect a similar suppression of the radiation.

The purpose of the present article is to gain some insight by exploring the particle creation phenomena that occur in a toy model consisting of a Domain Wall (DW) in AdS_4 with a CFT probing it (through gravity). The reason to choose this kind of source is that, once its gravitational effect is accounted for, a DW *is* a physical implementation of an accelerating mirror, hence one expects analogous particle production generically. The great advantage of this case is that this problem can be solved exactly both at 1-loop and at strong coupling, where it reduces to finding the 5D solution for a DW localized on the brane in the Karch-Randall model. Furthermore, in both cases it is possible to separate

the problem in two steps, by first neglecting the backreaction and then including it.¹ As a result, one can give a clear account of how the particle production is affected by A) the 't Hooft coupling (that is, whether the CFT is weakly or strongly coupled) and B) the backreaction of the CFT quantum effects themselves.

As we shall see, the most interesting case is when the DW is in asymptotically AdS_4 and its tension σ is small enough so that its proper acceleration is less than the AdS_4 curvature scale. We shall refer to these as *subcritical* DWs. Finding the amount of produced radiation and in fact the whole $\langle T_{\mu\nu} \rangle^{\text{CFT}}$ in the DW background can be done along the lines of [29], and for subcritical walls reduces to an ‘ordinary’ Casimir energy computation. We perform this explicitly at one loop for the two types of relevant boundary conditions (see section 2.2). As a result one obtains a certain amount of zero temperature CFT radiation in equilibrium with the AdS_4 boundary and the mirror (the DW), with an energy density that ‘piles up’ at a characteristic distance from the DW (see figure 1).

We then compare this to the non-perturbative strong coupling computation that one can infer from the 5D dual (section 3.1). Our first main result is that for every given boundary condition, the amount of radiation at weak and at strong coupling are of the same order, in some cases matching to within a few per cent (see figure 8). Hence, strong coupling effects do not substantially suppress the amount of radiation produced by DWs.

One important issue in this discussion concerns the boundary conditions. The Karch-Randall choice is specified by allowing the CFT to communicate at infinity with another field theory (the “CFT'”) with transparent boundary conditions [19–21]. In principle, this leaves a degree of arbitrariness in that we should specify the state for the CFT'. In our case, this becomes manifest because these boundary conditions are labelled by a continuous parameter representing whether the CFT' is probing a “Domain Wall'” (i.e., whether it is defined on a DW background). Of course, the natural choice is that the CFT' is in the ground state [19, 21] and that there is no DW' (more in general, that the CFT' lives on a space conformal to *pure* AdS_4). With these boundary conditions one always finds some radiation, roughly proportional to the DW tension σ . Strictly speaking, though, there is always a choice of boundary conditions for which no radiation is present. This happens if the CFT' is postulated to probe a DW' with tension opposite to that of ‘our’ DW. Clearly, though, this is not the most natural condition. In the 5D gravity dual, this corresponds to a 5D solution that is not asymptotically global AdS_5 but rather AdS_5 with a wedge removed.² Thus, it is also clear from the 5D perspective that this is not the relevant boundary condition and, rather, asymptotically globally AdS_5 (or the CFT' in the AdS_4 ground state) is preferred.

Regarding the backreaction, the most important point is that once the parameters *and* the boundary conditions in the two sides of the correspondence are appropriately mapped,

¹The gravity dual for the strongly coupled case without the backreaction, according to the ‘standard’ AdS/CFT correspondence, reduces to finding the 5D geometry whose boundary is conformal to the DW background.

²This situation has a direct parallel in the AdS_4 BH case with KR boundary conditions. The Uniform Warped Black String (even if stable) is not asymptotically AdS_5 . This would correspond to a state where the CFT' is directly probing a “BH'” with the same mass as the one probed by the CFT.

the two descriptions agree to leading order in the backreaction (which goes along the lines of previous claims [29–33]). This represents a quite solid check of the cutoff AdS/CFT correspondence and in particular of the holographic interpretation of the Karch-Randall model, stemming from the fact that it is based on exact solutions on the two sides. Indeed, all the previous checks of the 4Dgravity+CFT/braneworld equivalence are based either on perturbative arguments [9, 13, 19, 21, 22, 34–36], on the trace anomaly (and hence are insensitive to the actual vacuum state) [29–33, 37–39], or on lower dimensional models [40–43], while in some known exact solutions in the 5D side [44] the CFT computation is not known.

This match is especially remarkable for the ‘Bootstrap DW spacetimes’, a new kind of self-consistent solutions of the semiclassical Einstein equations that do not have a classical limit. In these solutions, the Casimir energy is nonzero because of the nontrivial geometry and the geometry is nontrivial because of the nonzero Casimir energy, in a way that is self-consistent and under control in the effective theory. It is perhaps not so surprising but yet quite revealing that these solutions also exist in the 5D dual, giving additional evidence that the braneworld models allow for a semiclassical 4D gravity interpretation.

The inclusion of the backreaction is also relevant for the massive gravity interpretation. As is well known, with KR boundary conditions for the CFT, the graviton acquires a mass² of order $N^2/(M_P^2 \ell_4^4)$ (where ℓ_4 is the AdS_4 curvature radius) while with reflecting conditions the graviton is massless [19, 21–23]. Since the graviton mass is ultimately a quantum effect, one expects that there is a trace of it in the the radiation produced by the DWs. The most natural manifestation of a graviton mass in our setup is in the form of a *screening* phenomenon, by which we mean that the effective gravitational effect due to the DW tension as perceived by far away observers may be smaller than expected. As we will see, the backreaction from $\langle T_{\mu\nu} \rangle^{\text{CFT}}$ precisely acts so as to screen the DW tension in this sense. This effect is not completely distinctive, though, since a Casimir energy is expected to be present generically for any choice of boundary conditions. However, it is possible to compare how much screening it leads to for each boundary conditions. Interestingly enough, we will find that for KR conditions there is always more such screening.

Finally, we shall comment on a more general point which gives a quite valuable insight, namely on the gravitational field of a Cosmic String (a relativistic codimension 2 brane) in AdS. This is relevant to our problem because in the 5D gravity side the DW localized on the brane is one such object, that is attached to a codimension 1 brane. Many of the properties of our 5D solutions simply follow from the peculiarities of isolated Cosmic String (CS) in AdS, so it proves very illustrative to momentarily dispose of the codimension 1 brane.

One might have expected that the solution representing a CS in AdS is simply given by AdS with a wedge removed, a space isometric to AdS that only differs in its global structure and where as usual all the gravitational effects would arise through the deficit angle only. It turns out, though, that the situation is much richer because, in contrast with the flat space case, in asymptotically AdS there is a number of possible boundary conditions. The locally AdS solution is asymptotically AdS minus a wedge. But for the same given CS tension, there is another solution, which we shall explicitly construct, that approaches asymptotically *global* AdS. There is of course a continuum of solutions interpolating between the two, but the asymptotically global AdS is clearly special, since the gravitational effect from the

CS is localized only in this case. Aside from a conical singularity, these solutions display a non-zero Weyl curvature, implying that with these boundary conditions, *Cosmic Strings produce tidal forces*. Not only that, they also generate a (repulsive) Newtonian potential. This is in fact the dual phenomenon lying behind the particle production by DWs in 4D.

The reason why there is more than one possible boundary condition in asymptotically AdS space is linked to the presence of a very interesting set of everywhere-regular vacuum solutions with $\Lambda < 0$, the so-called Hyperbolic AdS Solitons. These solutions approach asymptotically AdS with a wedge removed/added and have a nonzero Weyl curvature. In fact, these solitons can be viewed as (purely gravitational versions of) Cosmic Strings, since they are lumps of curvature localized around a codimension 2 region of spacetime and generate a deficit/excess angle. The globally AdS CS solutions of the previous paragraph are simply the superposition of an ordinary (material) CS and one of the AdS solitons. It is always possible to compensate the CS tension with the effective ‘tension’ carried by the gravitational soliton, in such a way that there is no deficit angle at infinity, where instead only the Weyl curvature is left.

This paper is organized as follows. Section 2 is devoted to the four dimensional side of the correspondence, having in mind a weakly coupled CFT. After a brief review of the connection between Domain Walls and accelerating mirrors, we discuss the quantum effects in DW backgrounds (that is ignoring the backreaction) in section 2.2. In section 2.2.1 we motivate and describe the two kinds of boundary conditions that we shall consider. In section 2.2.2 we perform the one loop computation of the Casimir energy on $AdS_3 \times S_1$, which is the background relevant for the subcritical walls. We include the backreaction in section 2.3. In section 2.3.1, we discuss the massive gravity interpretation and in section 2.3.2 we describe the Bootstrap DW spacetimes. Section 3 deals with the strong coupled CFT, first in section 3.1 without dynamical gravity, that is with no branes. We infer the strong coupling version of the Casimir energy in section 3.1.1. The dual with dynamical gravity, that is, the DW localized on the brane in the KR model is dealt with in section 3.2. Finally, in section 4 we discuss the gravitational effects of isolated codimension 2 branes in asymptotically AdS space, and we conclude in section 5.

2. CFT radiation from Domain Walls

In this section we discuss particle creation by Domain Walls in asymptotically AdS_4 assuming that the produced quanta belong to a weakly coupled four dimensional CFT. We perform our analysis in two steps: in section 2.2 we compute the amount of produced radiation ignoring its backreaction on the geometry, which we take into account in section 2.3.

2.1 Preamble: Domain Walls as accelerating mirrors

Let us start by briefly reviewing some aspects of the spacetimes produced by Domain Walls and their similarities with accelerating mirrors (a more detailed discussion in the same context can be found in [29]). For definiteness, we assume a negative cosmological constant and for the moment we ignore the CFT.

In the thin wall approximation, the stress tensor of a relativistic Domain Wall is

$$T_{\mu\nu}^{\text{DW}} = \sigma \delta(y) \text{diag}(1, -1, -1, 0)_{\mu\nu} \quad (2.1)$$

where σ is the tension, and y is the proper coordinate transverse to the wall. We shall consider the maximally symmetric configurations, where the metric can be foliated as

$$ds_4^2 = dy^2 + R^2(y) ds_\kappa^2 \quad (2.2)$$

where ds_κ^2 denotes the line element of a 3D Minkowski ($\kappa = 0$), de Sitter ($\kappa = 1$) or Anti de Sitter ($\kappa = -1$) spacetime of unit radius.

Assuming Z_2 symmetry across the DW, the Einstein equations imply that the extrinsic curvature of the DW $K_0 \equiv -(R'/R)|_{0+}$ is

$$K_0 = \frac{\sigma}{4M_P^2} \quad (2.3)$$

with $M_P^2 = 1/(8\pi G_N)$. This is an *acceleration* scale, namely the acceleration with which the DW recedes away from inertial observers. Hence, once gravity is ‘turned on’ a DW automatically accelerates fuelled by its own surface energy density, which gives a physical implementation of a moving mirror. Had we chosen an equation of state on the DW different from (2.1), the acceleration would be time dependent. But with only the tension term its proper acceleration is constant, leading to a model of a *uniformly* accelerated mirror. Needless to say, to actually make of the DW a real mirror that leads to particle production, one should specify appropriate boundary conditions for the propagating quantum fields on the wall. We comment on this below.

For the moment, let us mention some other properties of the DW spacetimes (2.2). The equations of motion also determine the (intrinsic) curvature scale $H_0^2 \equiv \kappa/R_0^2$ of the DW as

$$H_0^2 = K_0^2 - \frac{1}{\ell_4^2} \quad (2.4)$$

where $\ell_4^2 = -3M_P^2/\Lambda_4$ and $R_0 \equiv R(0)$. Hence, in the presence of a negative cosmological constant there is a ‘critical’ value of the DW tension

$$\sigma_c \equiv \frac{4M_P^2}{\ell_4}, \quad (2.5)$$

corresponding to an acceleration equal to $1/\ell_4$. For $|\sigma|$ smaller, equal or larger than σ_c , the DW worldvolume is AdS_3 , flat or dS_3 respectively. In each case, the ‘warp’ factor is

$$R(y) = \begin{cases} \ell_4 \cosh[(y_- - |y|)/\ell_4] & \text{for } \kappa = -1 \text{ (subcritical),} \\ \ell_4 e^{-|y|/\ell_4}, & \text{for } \kappa = 0 \text{ (critical),} \\ \ell_4 \sinh[(y_+ - |y|)/\ell_4], & \text{for } \kappa = 1 \text{ (supercritical).} \end{cases} \quad (2.6)$$

The integration constants y_\pm depend on σ , but they are irrelevant for the present discussion.

The point that we wish to stress here is that the spacetime given by (2.6) contains acceleration horizons for supercritical and critical cases only (at $y \rightarrow \infty$ in the latter case).

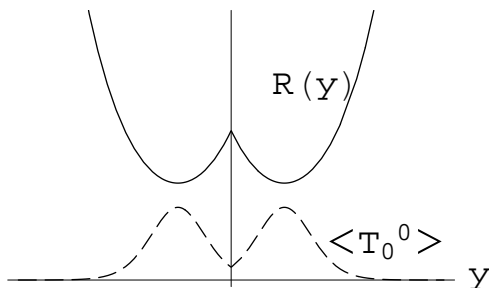


Figure 1: Schematic picture of a subcritical Domain Wall in AdS_4 , effectively acting as a uniformly accelerated mirror with acceleration smaller than $1/\ell_4$. The warp factor $R(y)$ (see case $\kappa = -1$ in (2.6)) bounces and grows exponentially. The expectation value of the stress tensor $\langle T_{\mu\nu} \rangle$ for the CFT does not vanish. In the equilibrium configuration, the energy density in the radiation peaks around the bounce of $R(y)$.

For subcritical walls, instead, the horizon is replaced by a bounce in the warp factor which takes place at finite distance from the wall.

In all cases the wall is accelerated, so one always expects some sort of particle production. Certainly, only when the acceleration K_0 exceeds $1/\ell_4$ the radiation from the wall may be *thermal*, with a temperature given by $H_0/2\pi = \sqrt{K_0^2 - 1/\ell_4^2}/2\pi$ [45, 46] (see [47] for a recent discussion). However, this does not mean that for subcritical walls there is no radiation but rather that it is simply not thermal. (We shall be a bit more precise about this in section 2.2) This does not exclude, for instance, that there is a Casimir energy, which is what we shall argue that happens in this case. The resulting situation is depicted in figure 1: for subcritical walls, the vacuum expectation value of the CFT energy density does not vanish and peaks at the location of the bounce. Arguably, one can view this as an equilibrium configuration where the produced radiation is in equilibrium with the wall and the AdS boundary.

Let us add finally that in the usual treatment of particle creation by moving mirrors, some sort of coupling between the quantum fields and the mirror is assumed, which can be encoded in the boundary condition for the fields at the location of the mirror. Here, we will assume that the CFT fields do not actually couple directly to the wall, so that on the DW we have transparent boundary conditions. As we shall see, even with this choice there is a non-trivial Casimir effect, because the global structure of the spacetime with the DW is slightly different than without it. Hence, this represents only a minimal choice, and the addition of any explicit coupling to the DW is not expected to change the picture qualitatively.

2.2 Quantum conformal fields on DW backgrounds

In this section we compute the expectation value (vev) of the stress tensor $\langle T_{\mu\nu} \rangle$ for conformally coupled fields of any spin in the Domain Wall spacetimes given by (2.6). For the moment, we take these as fixed backgrounds — the backreaction from $\langle T_{\mu\nu} \rangle$ on the geometry is deferred to section 2.3.

The vev of the stress tensor can always be split as

$$\langle T_{\mu\nu} \rangle^{\text{CFT}} = \langle T_{\mu\nu} \rangle^{(0)} + T_{\mu\nu}^{\mathcal{A}} \quad (2.7)$$

where the state-dependent part $\langle T_{\mu\nu} \rangle^{(0)}$ encodes the particle creation or vacuum polarization effects and is tracefree for conformal fields while $T_{\mu\nu}^{\mathcal{A}}$ is the state-independent anomalous contribution. On the spacetime (2.2), this only acts so as to renormalize the cosmological constant and the DW tension [29] and will be considered in more detail in section 2.3.

Further assuming that the vacuum state of the CFT respects the symmetries of the background (2.2) implies that $\langle T_{\mu\nu} \rangle^{(0)}$ is of the form

$$\langle T_{\mu}^{\nu} \rangle^{(0)} = P(y) \text{diag} \left(\frac{1}{3}, -\frac{1}{3}, -\frac{1}{3}, 1 \right)_{\mu}^{\nu}, \quad (2.8)$$

where P depends on the direction transverse to the DW only. Now, the local conservation of the stress-energy tensor demands that

$$P(y) = \frac{P_0}{R^4(y)}, \quad (2.9)$$

for some constant P_0 , which contains all the non-trivial particle production effects in this problem $\langle T_{\mu\nu} \rangle^{\text{CFT}}$. The value of P_0 depends on the kind of DW (i.e., on κ) and on the boundary conditions imposed on the CFT.

From (2.9), it is clear that when the spacetime contains a horizon, that is for critical and supercritical walls, there is no radiation of CFT quanta (that is, $P_0 = 0$). Otherwise, $\langle T_{\mu\nu} \rangle^{\text{CFT}}$ would diverge at the horizon, where $R(y) = 0$ [29].³ However, for subcritical walls $R(y)$ is nowhere zero and P_0 can be non-trivial. In the next Subsection we compute it at one-loop as a function of the DW tension, or equivalently its acceleration.

Note that in principle there can be self-consistent solutions (i.e. with the backreaction fully taken into account) for critical or supercritical walls where the horizon is replaced by a bounce as well. For these, P_0 can be nonzero — in fact it must be so because it is precisely the Casimir energy that supports the bounce. Given the key role played by the quantum effects in this kind of solutions, we shall call them ‘Bootstrap’ solutions. We discuss them further in section 2.3.2. At this point let us just mention that these solutions are perfectly trustable as long as P_0 is large enough and $\Lambda_4 < 0$.

Let us add that the distinction whether the stress tensor (2.8) should be viewed as describing the quanta created by the wall/mirror or simply as a Casimir energy is a bit obscure. Certainly, (2.8) appears quite different from the radiation perfect fluids commonly considered in cosmology — it is not isotropic and the equations of state are $p/\rho = -1$ and 3 in the longitudinal and transverse directions respectively. This suggests that (2.8) does not describe a *thermal* bath of radiation. However, when there is a horizon this is not the whole story. Let us accept momentarily for the sake of the argument the singular vacua with $P_0 \neq 0$ for supercritical DWs (alternatively, one could consider non-conformal fields, for which $\langle T_{\mu\nu} \rangle^{(0)}$ does not vanish and is regular at the horizon [51]). Neglecting

³This is confirmed by explicit computations at one-loop level [48–51].

any possible backreaction at the horizon, the stress tensor in the Milne region would be given by the analytic continuation of (2.8). Since in this continuation y becomes the time coordinate, in the Milne region $\langle T_{\mu\nu} \rangle^{(0)}$ becomes precisely an ordinary radiation perfect fluid, which one expects to describe a thermal distribution of quanta with temperature $\sqrt{K_0^2 - 1}/\ell_4^2/2\pi$ [45–47] despite looking non-thermal in the Rindler region (i.e. outside the light-cone defined by the DW). For subcritical walls there is no continuation to do, which agrees with the expectation that (2.8) does not describe thermal radiation. Still, it can be viewed as a kind of radiation in equilibrium with the wall and the AdS

Sub-critical walls. Let us consider in more detail the sub-critical walls (case $\kappa = -1$ in (2.6)), for which non-trivial quantum effects are expected. It is convenient to rewrite the metric (2.2) in terms of the conformal coordinate $\eta = \int_0^y dy'/R(y')$,

$$ds_4^2 = R^2(\eta) (d\eta^2 + ds_{AdS_3}^2) . \tag{2.10}$$

Given that $R(y)$ does not vanish and it grows exponentially for large enough y , the range of the conformal coordinate is finite,

$$\Delta\eta = \pi + 2 \arcsin \left(\frac{\sigma\ell_4}{4M_P^2} \right) . \tag{2.11}$$

Note that $\Delta\eta$ is conformally invariant (in other words, DW spacetimes with different tensions are *not* conformal to each other) and hence is a parameter that the CFT can be sensitive to. This quantity, then, is very convenient (e.g., it is conformally invariant) to characterize the DW spaces, and will play a key role in this discussion.

From (2.10) and (2.11), we see that every DW space is conformal to $I \times AdS_3$, where I denotes an interval of length $\Delta\eta$. Hence, the computation of $\langle T_{\mu\nu} \rangle$ is equivalent to a Casimir effect between hyperbolic ‘plates’ separated a distance $\Delta\eta$.

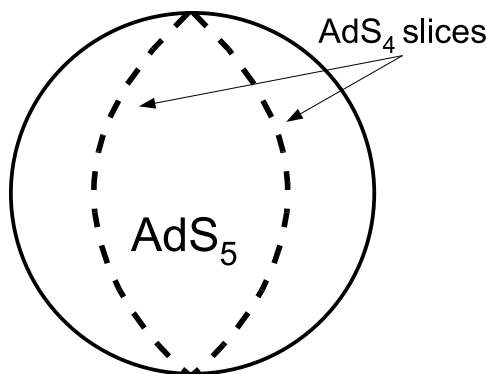
As is well known, the vevs of the stress tensor for conformal coupled fields in two conformally related spaces $g_{\mu\nu}$ and $\tilde{g}_{\mu\nu}$ satisfy

$$\langle T_{\mu\nu} \rangle = \frac{\sqrt{-\tilde{g}}}{\sqrt{-g}} \left[\langle \tilde{T}_{\mu\nu} \rangle - \tilde{T}_{\mu\nu}^A \right] + T_{\mu\nu}^A . \tag{2.12}$$

Comparing this with (2.7) we see that the first term in the rhs is the state-dependent part $\langle T_{\mu\nu} \rangle^{(0)}$. Hence, what we need to find is the state-dependent part of $\langle \tilde{T}_{\mu\nu} \rangle$ on $I \times AdS_3$. This again takes the form (2.8) with $\tilde{P}(y) = \tilde{P}_0/R_*^4$ where R_* is the radius of the AdS_3 factor and, from eq. (2.12), $\tilde{P}_0 = P_0$. In order to explicitly obtain P_0 , one could proceed with a direct mode-summation as was done in [52] for $AdS_4 \times I$. Here, though, we shall take a slightly quicker route that is allowed for by the kind of boundary conditions that we shall impose on the field theory.

2.2.1 Boundary conditions

Needless to say, the precise form of $P_0(\Delta\eta)$ depends on the boundary conditions on the DW and at infinity, that is, at the boundary of the interval I . As mentioned above, we shall take the minimalistic assumption that the CFT does not couple directly to the DW (i.e.,



$$\partial\text{AdS}_5 \approx \text{AdS}_4 \cup \text{AdS}_4 \approx S_1 \times \text{AdS}_3$$

Figure 2: Five dimensional Anti de Sitter space can be represented as a disk, with every point representing an AdS_3 . The boundary at infinity has a topology $AdS_3 \times S_1 \simeq S_3 \times R$. An AdS_4 slice ‘covers’ only half of the boundary. This motivates the Karch-Randall boundary conditions.

the coupling is through geometry that it produces only), which can be stated as imposing transparent boundary conditions on the wall.

Because the boundary of AdS is timelike, to proceed we also need to specify the boundary conditions at infinity. As explained in [19, 21–23], these play a key role in the dual of the Karch-Randall (KR) model [18], in particular to obtain the graviton mass. Let us describe next the two types of boundary conditions that we shall consider in this paper.

Karch-Randall boundary conditions. In order to compare the 1-loop with strong coupling results of section 3, we shall impose the boundary conditions that are built-in in the Karch-Randall (KR) model [18]. The so-called KR boundary conditions are such that the CFT communicates at infinity with an additional conformal field theory (which we shall refer to as the CFT’) living on an adjacent copy of AdS_4 , with transparent boundary conditions [18, 19, 21, 23].

In our problem, this means that we have to glue the interval I to another one I' spanned by, say, η' . Since the boundary of the two intervals is common, this naturally defines a circle $S_1 = I \cup I'$ (we will call θ the coordinate along S_1). ‘Transparent’ boundary conditions at the common boundary of I and I' then translates into (anti)periodic boundary conditions on the S_1 . Intuitively, this is because the full boundary of AdS_5 is $R \times S_3$, which is equivalent to $AdS_3 \times S_1$, or to two AdS_4 spaces sharing their common boundary, as depicted in figure 2.

In practice, then, computing the Casimir energy on $AdS_3 \times I$ with KR boundary conditions is equivalent to computing it on $AdS_3 \times S_1$,

$$R_*^2 (d\theta^2 + ds_{AdS_3}^2) , \tag{2.13}$$

(the overall scale R_* is going to be irrelevant) with the length of the circle given by

$$\Delta\theta = \Delta\eta + \Delta\eta' . \tag{2.14}$$

In this article, we will assume periodic boundary conditions for the bosons and antiperiodic for the fermions. In section 3.1.1 we shall comment on the case when the fermions are periodic.

Note that the transparency of the assumed boundary conditions at the AdS_4 boundary implies that the Casimir energy P_0 is going to be really a function of $\Delta\theta$ and it will depend on $\Delta\eta$ through eq. (2.14). Hence, the actual form of $P_0(\Delta\eta)$ is subject to the choice of boundary condition encoded by $\Delta\eta'$, which hiddenly entails a choice of the state for the CFT'. Of course, the natural choice is that the CFT' is in its ground state [19, 21], which demands in particular that it is not directly probing any “Domain Wall' ” and hence,

$$\Delta\eta' = \pi . \tag{2.15}$$

With this boundary conditions, then the Casimir energy is going to be

$$P_0^{\text{KR}}(\Delta\eta) \equiv P_0(\Delta\theta = \Delta\eta + \pi) \tag{2.16}$$

(we defer to section 2.2.2 the computation of $P_0(\Delta\theta)$). As we shall see, eq. (2.15) is the only choice that leads to no particle production ($P_0 = 0$) in the absence of the DW.

By the same token, this also means that there is always a state (a choice of $\Delta\eta'$) such that there is no particle production for any DW tension. This will be trivially accomplished choosing $\Delta\eta' = 2\pi - \Delta\eta$ simply because as we will see, $P_0(\Delta\theta = 2\pi) = 0$. However, this should not be ascribed to any strong coupling effect, of course. Rather, in these states the boundary conditions for the CFT' are quite exotic — it is probing the presence of a DW' with tension equal to $-\sigma$.

The choice of vacuum for the CFT' is thus an essential ingredient of the computation. In the gravity picture, it is dual to the choice of boundary conditions in the bulk and the natural condition is going to be that the bulk is asymptotically *global* AdS_5 . As we shall see, this corresponds precisely to the state where the CFT' is in the ground state, eq. (2.15), or more precisely that the geometry that it probes is conformal to pure AdS_4 . This goes very much along the lines of what was observed in [43] for the shock waves in an AdS_3 brane, where two solutions with different asymptotics in the bulk correspond to two rather different states of the CFT.

Reflecting boundary conditions. Without much additional effort, it is also possible to identify the form of $\langle T_{\mu\nu} \rangle$ for a certain type of reflecting boundary conditions. In our setup, reflecting means that on the boundary of I the fields obey either Dirichlet or Neumann boundary conditions. Given that I has two boundaries (corresponding to the two halves of the $R \times S_2$ boundary of AdS_4), and that the CFT has a number of fields of different spin, there are in principle several different kinds of reflecting boundary conditions. The type that we will consider is the one that can be obtained as a particular case of KR conditions by taking the CFT' sector to be identical to the CFT and letting it probe a replica of ‘our’ DW. In other words, we simply take

$$\Delta\eta' = \Delta\eta , \tag{2.17}$$

and so the Casimir energy is

$$P_0^{\text{refl}}(\Delta\eta) \equiv P_0(\Delta\theta = 2\Delta\eta) . \tag{2.18}$$

The reason why this can be viewed as reflecting boundary conditions (for the purpose of computing $\langle T_{\mu\nu} \rangle$) is the following. As depicted in figure 3, we can always expand the modes on the S_1 in terms of sines and cosines and choosing appropriately the phase, we have modes that are either Neumann (N) or Dirichlet D at the two equatorial points of the S_1 (which coincide with the boundary of I). Schematically, a periodic field can be viewed as a sum of direct products of NN and DD fields:

$$\psi_{S_1}^P = \frac{1}{\sqrt{2}} \left(\phi_I^{\text{NN}} \otimes \phi'_{I'}^{\text{NN}} + \phi_I^{\text{DD}} \otimes \phi'_{I'}^{\text{DD}} \right) .$$

Similarly, for the antiperiodic fields one as

$$\psi_{S_1}^{\text{AP}} = \frac{1}{\sqrt{2}} \left(\phi_I^{\text{ND}} \otimes \phi'_{I'}^{\text{DN}} + \phi_I^{\text{DN}} \otimes \phi'_{I'}^{\text{ND}} \right) .$$

These superpositions are nothing but the one noted in [21], where it was argued that the KR boundary conditions correspond to a mixture with equal weights of the modes of $R \times S_3$ that are either symmetric or antisymmetric under the reflection that maps one hemisphere of the S_3 into the other. Indeed, in our notation the NN \times NN and DN \times ND modes are symmetric while the DD \times DD and ND \times DN modes are antisymmetric.

The main lesson of [19] is that a superposition of modes such as above can give the graviton a mass. The key element of the computation is a crossed term in the graviton self-energy $\sim \langle T_{\mu\nu} T_{\rho\sigma} \rangle$ which vanishes unless both symmetric and antisymmetric modes are present. However, here we shall only compute the one point function $\langle T_{\mu\nu} \rangle$, and this cannot contain crossed terms (at the quadratic level, that is in the 1-loop approximation). In other words, the $\langle T_{\mu\nu} \rangle$ for KR (anti)periodic boundary conditions and for the appropriate combination of D and N conditions on I should be the same. More precisely, one should have

$$P_{0(S_1)}^P = P_{0(I)}^{\text{NN}} + P_{0(I)}^{\text{DD}} \quad \text{and} \quad P_{0(S_1)}^{\text{AP}} = P_{0(I)}^{\text{ND}} + P_{0(I)}^{\text{DN}} .$$

This equivalence can of course be broken when the CFT is interacting, so in that case by ‘reflecting’ boundary conditions we will just mean the KR ones with the choice (2.17).

Finally, notice an important difference that we can already foresee between the Casimir energies with KR and reflecting boundary conditions, eqs. (2.16) and (2.18). Since, as we will see, $P_0(\Delta\theta)$ has a simple zero at $\Delta\theta = 2\pi$ and for small DW tension $\Delta\eta = \pi + O(\sigma)$, one automatically obtains that for small σ

$$P_0^{\text{refl}} \simeq 2P_0^{\text{KR}} ,$$

which does not seem surprising after all. This turns out to be of some relevance for the interpretation of our results in terms of massive gravity, see section 2.3.1.

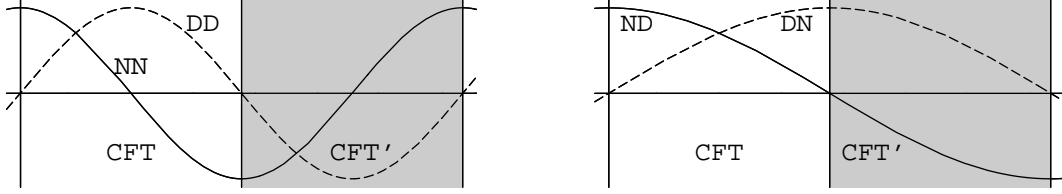


Figure 3: First excited modes along the circle in $AdS_3 \times S_1$ for periodic (left) and antiperiodic (right) boundary conditions. The unshaded (shaded) region represent the spaces where the CFT (CFT') are defined, both of them of the form $AdS_3 \times I$.

2.2.2 Casimir energy on $AdS_3 \times S_1$ at weak coupling

Let us now evaluate the Casimir energy on $AdS_3 \times S_1$ at one loop for arbitrary conformally coupled fields. This can be easily achieved by exploiting the conformal invariance of the field theory and the conformal properties of the background.

Writing the AdS_3 line element in horospheric coordinates $ds_{AdS_3}^2 = (dz^2 + dx^2 - dt^2)/z^2$, one readily sees that the metric (2.13) is conformal to the spacetime created by a Cosmic String (CS)

$$z^2 d\theta^2 + dz^2 + dx^2 - dt^2, \quad (2.19)$$

which has a deficit angle $2\pi - \Delta\theta$. The Casimir energy density in this spacetime has been widely studied [53–56] and these results can easily be transformed to the case of our interest. Since in the CS space the circles defined by θ are contractible, in these computations the fermions obey antiperiodic boundary conditions, which is what we need.

For the CS spacetime, the anomaly term vanishes and $\langle T_{\mu\nu} \rangle$ is of the form

$$\langle T_{\mu\nu} \rangle^{(CS)} = \frac{P_0^{(CS)}}{z^4} \text{diag} \left(\frac{1}{3}, -\frac{1}{3}, -\frac{1}{3}, 1 \right)_{\mu\nu}. \quad (2.20)$$

Using again (2.12), one realizes that $P_0^{(CS)} = P_0$ so we can straightforwardly identify the Casimir energy. For a collection of N_0 conformal scalars, $N_{1/2}$ Majorana fermions and N_1 vectors, the result is [54]

$$P_0^{1-loop} = \frac{1 - \nu^2}{1920\pi^2} [4N_0(\nu^2 + 1) + N_{1/2}(7\nu^2 + 17) + 8N_1(\nu^2 + 11)] \quad (2.21)$$

where $\nu = 2\pi/\Delta\theta$.

For $\mathcal{N} = 4$ Super-Yang-Mills (SYM) with N colours, it is convenient to introduce the rescaled Casimir energy

$$p \equiv \frac{32\pi^2}{3N^2} P_0, \quad (2.22)$$

which measures the Casimir energy per colour degree of freedom. The field content is

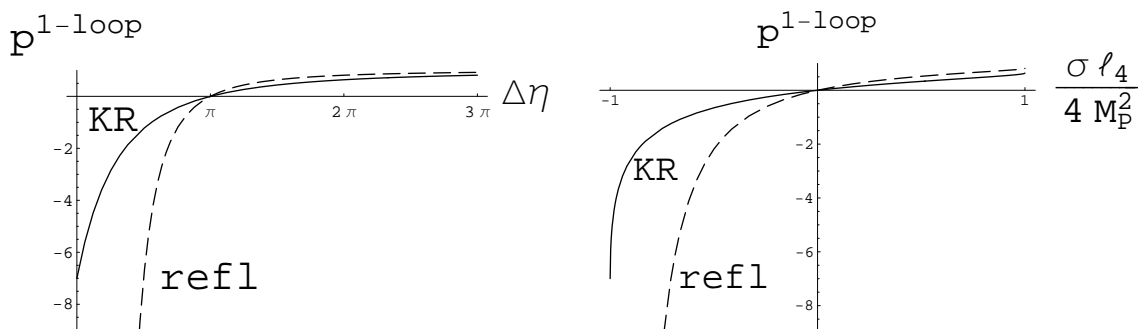


Figure 4: Left panel: Casimir energy (density) for the CFT as a function of the conformal interval $\Delta\eta$ for KR boundary conditions (solid line) and for reflecting boundary conditions (dashed line). These results are obtained from (2.23) taking $\Delta\theta = \pi + \Delta\eta$ or $\Delta\theta = 2\Delta\eta$ for KR or reflecting boundary conditions respectively. Right panel: The same, as a function of the DW tension σ or, equivalently, its acceleration. Note that for small σ the Casimir energy with reflecting boundary conditions is twice as much that with KR conditions.

$N_0 = 6N^2$, $N_{1/2} = 4N^2$ and $N_1 = N^2$, so one finds⁴

$$p^{1-loop}(\Delta\theta) = \left(1 - \left[\frac{2\pi}{\Delta\theta}\right]^2\right) \left(1 + \frac{1}{3} \left[\frac{2\pi}{\Delta\theta}\right]^2\right). \quad (2.23)$$

As advanced, this vanishes for $\Delta\theta = 2\pi$ (it does so for each spin). For small $\Delta\theta$, it behaves as a usual Casimir force $\sim 1/\Delta\theta^4$.

Once we know $p^{1-loop}(\Delta\theta)$, we can obtain it as a function of the conformal interval $\Delta\eta$ for KR and reflecting boundary conditions by means of (2.16) and (2.18) respectively. Also, since $\Delta\eta$ depends on the DW tension σ through (2.11), it is also straightforward to obtain p^{1-loop} as a function of σ or alternatively its acceleration. These results are plotted in figure 4.

Thus, we find that the vacuum polarization induced by subcritical walls (may it be viewed just as a Casimir effect or as a cold bath of radiation created by a mirror with acceleration $K_0 < \ell_4$) is, as expected, nonzero. As we will explain in section 4, the phenomenon dual to this in the gravity side is the fact that pure-tension codimension-2 branes generate a long range Weyl curvature (aside from a deficit angle) in AdS space.

It is also possible to compute $p(\Delta\theta)$ at strong 't Hooft coupling (still ignoring the back-reaction) using the 'standard' methods of AdS/CFT, that is, without dynamical gravity in the 4D side. We will do this in section 3.1.1, but let us advance that the difference with respect to the weak coupling result (2.23) is quite small (see figure 8). Hence, we conclude that strong coupling does not prevent the DW from radiating CFT quanta (on the contrary, we will find that for positive DW tension, the amount of radiation is actually

⁴The result (2.23) can also be obtained by analytical continuation of the thermal state of the CFT on the Hyperbolic plane [57] with temperature $1/\Delta\theta$ (which is dual to the hyperbolic Schwarzschild AdS₅ black Hole [57]). This is for granted because both configurations have the same Euclidean section.

larger for $\lambda \rightarrow \infty$). One may wonder whether this conclusion can be changed once we introduce the backreaction. As we shall soon see, it will not.

2.3 Including the backreaction

Let us now consider the full problem, since the stress tensor that we have just computed (see eqs. (2.8), (2.9) and (2.22)) will feed back and modify the geometry that we assumed (2.6). Our goal is to self-consistently solve the semiclassical Einstein's equations

$$M_P^2 G_{\mu\nu} = -\Lambda_4 g_{\mu\nu} + T_{\mu\nu}^{\text{DW}} + \langle T_{\mu\nu} \rangle^{\text{CFT}} . \quad (2.24)$$

In the thin wall approximation, we can separate the problem by first working out the exterior of the DW and then gluing the two sides by means of an appropriate matching condition. Away from the DW, the semiclassical equations (2.24) reduce to a ‘Friedman’ equation, that can be conveniently written as [29]⁵

$$\frac{R'^2 - \kappa}{R^2} = \frac{1}{\ell_4^2} - \frac{\ell_5^2}{4} \left(\frac{R'^2 - \kappa}{R^2} \right)^2 + \frac{\ell_5^2}{4} \frac{p(\Delta\eta)}{R^4} \quad (2.25)$$

where p is defined in (2.22) and we introduced

$$\ell_5^2 = \frac{N^2}{8\pi^2 M_P^2} . \quad (2.26)$$

As is obvious from (2.25), ℓ_5 is the scale that controls the backreaction and because of the large N limit assumed, it is much larger than the Planck scale. In fact, ℓ_5^2 is the gravitational version of the 't Hooft coupling, and is the relevant scale because it is the combination that enters in the CFT loops. This is also one reason why it plays the role of the inverse cutoff of the theory [6, 58, 59]. Needless to say, in the gravity dual ℓ_5 is the curvature radius of AdS_5 .

On the other hand, the matching condition also receives a correction from the anomaly [29],

$$K_0 \left(1 + \frac{1}{6} \ell_5^2 \left(K_0^2 - \frac{3\kappa}{R_0^2} \right) \right) = \frac{\sigma}{4M_P^2} \quad (2.27)$$

where as before $K_0 = -(R'/R)_{0+}$ is the extrinsic curvature of the DW.

Let us emphasize that eqs. (2.25) and (2.27) describe the whole CFT + gravity system coupled to the DW also beyond the 1-loop or the planar approximations (in the maximally symmetric configuration). Indeed, the form (2.8) of the stress tensor is fixed by the symmetries and conformal invariance, and the conformal anomaly does not receive higher loop corrections for $\mathcal{N} = 4$ SYM. The dependence on the 't Hooft coupling $\lambda = g_{\text{YM}}^2 N$ and the corrections from non-planar diagrams enter only in the functional form of $p(\Delta\eta)$. As we have seen, for subcritical walls this is given by (2.23), (2.14) at $\lambda = 0$. In section 3.1.1, we shall obtain the non-perturbative form of p at strong coupling ($\lambda \rightarrow \infty$) to leading order

⁵The second piece in the r.h.s. of (2.25) is the anomaly term. Here, we assume that there is no contribution from the counterterm $\sqrt{-g}R^2$ as it breaks conformal invariance.

in $1/N$ using ‘standard’ AdS/CFT technology. As we will see, they differ very little (see eq. (3.5) or figure 8), so to fix ideas we shall stick to the weak coupling expression (2.23).

Hence, for every given value of λ (and of N , in general), $p(\Delta\eta)$ is a fixed function that depends on the geometry only through $\Delta\eta$. Then, one way to find the self-consistent solutions of (2.25) and (2.27) in general is as follows. We substitute momentarily $p^{1-loop}(\Delta\eta)$ by a constant, call it p_* . Then, it is straightforward to integrate (2.25), (2.27) and the resulting warp factor $R_*(y)$ depends parameterically on p_* , as well as on the dimensionless quantities

$$\epsilon \equiv \left(\frac{\ell_5}{\ell_4}\right)^2$$

(this is the relevant dimensionless gravitational coupling constant) and

$$\tilde{\sigma} \equiv \frac{\sigma\ell_4}{4M_P^2}.$$

Then, we compute the conformal interval $\Delta\eta_*(p_*; \epsilon, \tilde{\sigma})$ for $R_*(y)$,

$$\Delta\eta_*(p_*; \epsilon, \tilde{\sigma}) \equiv 2 \left[\int_{R_b}^{\infty} + \text{sign}\sigma \int_{R_b}^{R_0} \right] \frac{1}{R} \frac{dR}{R'(R)} \tag{2.28}$$

where R_b is the warp factor at the bounce and $R'(R)$ is obtained from (2.25). Then, the self-consistent solutions at 1-loop in the conformal fields must satisfy

$$\Delta\eta_* \left[p^{1-loop}(\Delta\eta); \epsilon, \tilde{\sigma} \right] = \Delta\eta. \tag{2.29}$$

This defines the relation between $\Delta\eta$ and the tension that fully incorporates the backreaction (it is built-in that it reduces to (2.11) for $\epsilon = 0$).⁶ Note that combining (2.29) and (2.14), the same condition can be cast as

$$\Delta\theta^{1-loop}(p) = \Delta\eta_* [p; \epsilon, \tilde{\sigma}] + \Delta\eta', \tag{2.30}$$

where $\Delta\theta^{1-loop}(p)$ denotes the inverse of (2.23), and it is transparent that this determines the Casimir energy as a function of the tension, the backreaction parameter and the boundary conditions, $p = p(\tilde{\sigma}, \epsilon, \Delta\eta')$ (since the l.h.s. is a function of p only). In the form (2.30), the self-consistency condition has a straightforward geometrical interpretation in the 5D dual.

This procedure works for values of ℓ_5 (in principle) arbitrarily large, so one could keep track of the backreaction to all orders in ℓ_5 . Here, though, we shall not pursue this task because ℓ_5 is the inverse cutoff, so the only trustable solutions are those where ℓ_5 is small as compared to any other scale and we shall content ourselves with the backreaction from $\langle T_{\mu\nu} \rangle$ on the geometry to the leading order, i.e., $O(\ell_5^2)$. Note that this will not prevent us from finding new solutions that exist only because of the backreaction and which still lie within the validity of the effective theory. These solutions necessarily have no classical limit

⁶Needless to say, the extension of (2.29) for any value of λ is just given by the same relation but with the corresponding form of the Casimir energy $p^\lambda(\Delta\eta)$ as the first argument in the r.h.s.

(typically when sending $\ell_5 \rightarrow 0$ the curvature scales grow beyond $1/\ell_5$), and we shall call them ‘Bootstrap’ Domain Wall spacetimes. Examples of these solutions will be discussed in section 2.3.2.

Before addressing the DW spacetimes, let us briefly see what happens in the absence of any DWs. An important question that we can already answer is whether in the absence of DWs, the solution of (2.25), (2.27) is unique. As it turns out, this is not entirely trivial and in fact strongly depends on the form of the Casimir term $p(\Delta\eta)$, that is, on the field theory and on the boundary conditions. It is easy to check that for $\mathcal{N} = 4$ SYM and KR boundary conditions with $\Delta\eta' = \pi$ (in the $\kappa = -1$ case), only pure AdS (that is, $\Delta\eta = \pi$, or equivalently $p = 0$) is a solution of equation (2.29). (Strictly speaking, there are solutions other than $p = 0$ but only if $\ell_5 \gtrsim \ell_4$, so they cannot be trusted.⁷ In the gravity side these solutions will not present, of course.) For reflecting boundary conditions one has a similar situation.

2.3.1 Massive gravity interpretation

Going back to the DW case, let us see in full detail how the presence of $\langle T_{\mu\nu} \rangle$ affects the geometry to leading order. Given that in the presence of a subcritical DW the Casimir energy is already non-zero at zeroth order and that this enters in (2.25) suppressed by ℓ_5^2 , we only need to find the modification of the warp factor $R(y)$ to order ℓ_5^2 and this will represent the self-consistent solution of (2.25) to leading order in ℓ_5^2 . In the process, we shall give the massive gravity interpretation of these solutions in terms of a particular pattern of screening of the DW tension.

Already from the form of eqs. (2.25) and (2.27), it is clear that generically some screening takes place at two distinct levels. The first comes from the boundary condition on the DW and so is local. The anomalous contribution acts so as to effectively renormalize the DW tension [29]. We can define the *effective* tension that is generating the acceleration scale K_0 close to the wall (2.27) as $\sigma + \delta\sigma_{\text{local}} \equiv 4M_P^2 K_0$. We shall use as a measure of the screening the ratio $\delta\sigma/\sigma$. Then, substituting the zeroth order values of K_0 and R_0 in the $O(\ell_5^2)$ terms of (2.27) one obtains

$$\frac{\delta\sigma_{\text{local}}}{\sigma} = -\frac{\epsilon}{6} (3 - 2\tilde{\sigma}^2) , \tag{2.31}$$

which is negative for subcritical walls. Hence, the acceleration produced by the DW is actually smaller than the classical value (2.3). This looks like a genuine screening phenomenon, similar to that found in [60] for the DGP model [61]. However, it is dubious that we should ascribe it to the fact that the graviton is massive in this model because it is independent of the boundary conditions chosen for the CFT.⁸ Rather, this kind of screening is associated

⁷One may wonder if this conclusion holds for any free conformal theory. With arbitrary N_0 , $N_{1/2}$ and N_1 , the anomaly will contain in general a $\square R$ term (which would render (2.25) higher derivative) but this can always be cancelled by appropriately choosing the $\sqrt{-g} R^2$ counterterm. With this choice, it is also possible to show that there is no choice of N_0 , $N_{1/2}$ and N_1 that generates self-consistent solutions other than $p = 0$ (with small ϵ .)

⁸Besides, this effect is also present even for $\Lambda_4 \geq 0$. However, it is intriguing that in these cases the 3 in (2.31) is replaced by 0 or -3 , thus obtaining *anti*-screening instead.

to the fact that the trace anomaly captures some of the short-distance properties of the 5D dual. In terms of the gravity dual, this screening arises because the DW is *also* sourcing a deficit angle in the bulk [29].

However, this is not the whole story because the Casimir energy can also contribute to change the effective tension as measured far away from the DW. It is not immediately obvious to us how to rigorously define the notion of the DW tension measured at infinity, so in the following we will resort to a convenient coordinate system where the identification of the effective tension at infinity seems natural. This is given by a ‘Schwarzschild’-like coordinate, where the metric is

$$ds_4^2 = \ell_4^2 \left(\frac{dz^2}{F(z)} + F(z) ds_{AdS_3}^2 \right) \tag{2.32}$$

with $F \equiv (R/\ell_4)^2$. In this gauge, the ‘classical’ background (2.6) (with $\kappa = -1$) is

$$F_c(z) = 1 + (|z| - z_0)^2 \tag{2.33}$$

where

$$z_0 \equiv \frac{\tilde{\sigma}}{\sqrt{1 - \tilde{\sigma}^2}}. \tag{2.34}$$

The advantage of this gauge is that the different contributions to the Newtonian potential ($F - 1$) are simply added up. Expanding (2.33), one identifies the usual quadratic potential due to the cosmological constant, and a the linear potential $-2z_0|z|$ generated by the wall at $z = 0$. In terms of this metric potential, then, a screening of the DW tension translates into a modification of the coefficient of the term linear in z .

To leading order in the backreaction the solution can be separated as

$$F(z) = F_c(z) + \delta F(z)$$

where δF is of order ϵ . Introducing this expansion in the equations of motion (2.25), (2.27) and isolating the $O(\epsilon)$ terms leads to the following equations for δF

$$\frac{1}{2} \frac{F'_c}{F_c} \delta F' - \frac{\delta F}{F_c} = \frac{\epsilon}{4} \left(\frac{p}{F_c^2} - 1 \right) \tag{2.35}$$

$$\left(\frac{\delta F'}{F'_c} - \frac{1}{2} \frac{\delta F}{F_c} \right) \Big|_{z=0^+} = \frac{\epsilon}{2} \left(1 - \frac{2}{3} \tilde{\sigma}^2 \right) \tag{2.36}$$

where a prime denotes differentiation with respect to z . The solution is

$$\delta F = \frac{\epsilon}{12} \left\{ 3 - (z - z_0)(3z - (6 + z_0^2)z_0) - 3p [1 - (z - z_0)(\arctan(z - z_0) + \arctan z_0)] \right\} \tag{2.37}$$

Expanding this for $z \rightarrow \infty$, one identifies that the effective tension perceived at infinity differs from σ by

$$\frac{\delta\sigma_\infty}{\sigma} = \frac{(\delta z_0)_\infty}{\tilde{\sigma} \frac{dz_0}{d\tilde{\sigma}}} = \epsilon \left\{ \frac{1}{8} - \frac{3 - 2\tilde{\sigma}^2}{6} + \frac{(1 - \tilde{\sigma}^2)^{3/2}}{16\tilde{\sigma}} \left(\pi + 2 \arctan \frac{\tilde{\sigma}}{\sqrt{1 - \tilde{\sigma}^2}} \right) p \right\}. \tag{2.38}$$

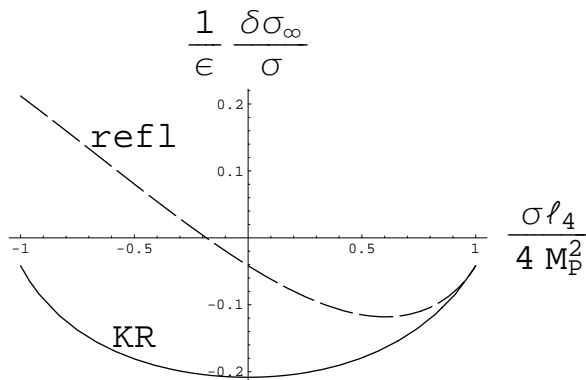


Figure 5: The amount of screening of the DW tension measured at infinity, eq. (2.38), enhanced by a factor $1/\epsilon$. Clearly, KR boundary conditions give more screening ($\delta\sigma_\infty/\sigma$ is more negative) than the reflecting ones.

The first contribution in the curly brackets comes from the anomaly term away from the DW which, even for $p = 0$, renormalizes the AdS curvature $\ell_4^{-2} \rightarrow (1 - \epsilon/4)\ell_4^{-2}$. The second contribution is precisely the local screening term (2.31) that takes place at the DW location itself as we discussed. The remaining p -dependent term is the truly non-local effect, due to the Casimir stress.

We plot the total effect at infinity $\delta\sigma_\infty/\sigma$ both for KR and reflecting boundary conditions in figure 5. It is encouraging to see that for KR conditions one always has screening ($\delta\sigma_\infty/\sigma < 0$). For reflecting conditions, one can have either anti-screening or screening, depending on the value of σ . Furthermore, it is safe to say that one has always *more* screening with the KR choice (that is, $\delta\sigma_\infty/\sigma$ is more negative in this case). It is of course quite tempting to ascribe this phenomenon to the fact that the graviton is massive with the KR conditions.

The reason why $\delta\sigma_\infty/\sigma$ is more negative for KR conditions can be traced back to the form of the Casimir energy $p(\sigma)$. In particular, it relies on 1) p is larger (in magnitude) for reflecting boundary conditions and 2) the sign of p is the same as that of σ . Thus, in any field theory where these two properties hold, KR boundary conditions will give more screening.

Let us finish by mentioning that even though for KR conditions the graviton is massive [18, 19, 21–23, 36] with a mass $m_g^2 \sim \epsilon/\ell_4^2$, it seems that (for the DWs) we do not find any trace of a ‘Compton wavelength’ scale in the self-consistent solution. Indeed, the radiation ‘halo’ is peaked around the bounce with a typical (proper) width of order ℓ_4 , as pictured in figure 1. Hence, the largest modification of the geometry occurs in this region, and it is natural to expect that the non-local screening basically occurs there. However, the bounce is a proper distance

$$y_* \simeq \ell_4 \operatorname{arctanh} \left(\frac{\sigma \ell_4}{4M_P^2} \right) + \mathcal{O}(\epsilon) \tag{2.39}$$

from the wall. This scale has little to do neither with the Compton wavelength $\ell_4/\sqrt{\epsilon}$ nor

the scale at which the deviations from massless AdS gravity $\sim \ell_4/\epsilon$ were found for the shock wave solutions [44]. The distance between the wall and the (center of the) radiation cloud, y_* , is larger than the width of the radiation cloud itself only for walls already quite close to critical, and it becomes larger than m_g^{-1} (as in the shock wave case) only for tensions exponentially close to critical. For moderate tensions, though, all forms of the screening take place within one curvature radius, $\sim \ell_4$.

Hence, at least for the DWs, the graviton mass does not manifest itself by displaying a different behaviour in the metric at a certain length scale related to the mass. This might be due to the large amount of symmetry that we have assumed, and hence might be only a particular feature of the maximally symmetric DWs. Instead, the presence of a larger screening for KR boundary conditions as summarized in figure 5 seems a more clear indication that gravity is massive in this case.

2.3.2 Bootstrap Domain Wall spacetimes

Let us now discuss a new kind of asymptotically AdS solutions that appear thanks to the backreaction from the Casimir energy itself. These solutions have no classical counterpart, and we will call them ‘Bootstrap DW spacetimes’. As we will see, some of these solutions (those with a positive tension DW) display a bounce that is supported by the Casimir energy.

In these solutions, the link between whether the tension is sub- or super-critical and the sign of the curvature of the DW worldsheet (κ) is lost, simply because what determines κ is now the balance between the DW tension against a combination of Λ_4 and the Casimir energy density next to the DW. Hence, from now on, we shall call the solutions with $\kappa = 0$ ‘planar’ and those with $\kappa = 1$ ‘inflating’.

As argued in [29], the reason why such solutions do not exist with $\Lambda_4 \geq 0$ is that in order that the curvature scale at the bounce is below the cutoff, p must be large and negative. As we have seen in section 2.2.2, this can be accomplished if the conformal interval $\Delta\eta$ is small enough. But this is impossible in an asymptotically flat or de Sitter space (because $R(y)$ does not grow fast enough at infinity), so the only solutions of this form have the direction transverse to the DW compact (with a finite *proper* length), and would represent a DW in a ‘cage’. For $\Lambda_4 < 0$, the situation is very different because AdS acts as the cage. In other words, a finite conformal interval does not imply that the space is compact in this case.

Going back to $\Lambda_4 < 0$, from (2.25), the bounce occurs at

$$R_b^2 = \frac{\ell_4^2}{2} \left(-\kappa + \sqrt{(1 + \epsilon)\kappa^2 - \epsilon p} \right) . \tag{2.40}$$

For inflating walls, this is only larger than the cutoff $\ell_5^2 = \epsilon\ell_4^2$ if $|p| \gtrsim 1/\epsilon$. In these cases the solutions can be trusted. For planar walls, (2.40) is larger than ℓ_5 even if p is of order one, but this is only a manifestation that this case represents the limit $p \rightarrow -\infty$, $R_b \rightarrow \infty$ of the $\kappa = 1$ case. In fact, for $\kappa = 0$ the value of $R(y)$ at a given point has no meaning because it can be scaled away by a change of coordinates. In this case, all curvature invariants are of order $1/\ell_4$ irrespective of p .

Let us consider the planar case ($\kappa = 0$) in more detail (the following discussion parallels in many respects that of [62] in a five dimensional context; similar arguments apply to inflating walls, but we shall leave this case for the future). As we shall now see, when the backreaction from the Casimir effect is included, there is always a range of DW tensions for which there are self-consistent solutions where the DW is planar but the tension is subcritical.

Since the radiation term in (2.25) is at most comparable to Λ_4 (close to the bounce), to leading order in ϵ we can safely neglect the anomaly term. Hence, the Friedman equation reduces to

$$\frac{R'^2}{R^2} \simeq \frac{1}{\ell_4^2} + \frac{\ell_5^2}{4} \frac{p}{R^4}. \quad (2.41)$$

Note that in the planar DW case, we can always rescale the coordinates so that we can fix R at will at one point. This should translate in (2.41) as a scaling symmetry $R \rightarrow \gamma R$. The radiation term does have this symmetry because for $\kappa = 0$ there is only one scale ($\Delta\eta$), so by conformal invariance the Casimir must take the form $p \sim 1/(\Delta\eta)^4$, hence it scales like $p \rightarrow \gamma^4 p$.

The solution of (2.41) is

$$R(y) = R_b \cosh^{1/2}[(2|y| - y_0)/\ell_4], \quad (2.42)$$

where now $R_b = (-\epsilon p/4)^{1/4} \ell_4$. The integration constant y_0 is fixed by the junction condition at the DW, which for planar walls reads

$$K_0 \left(1 + \frac{1}{6} \ell_5^2 K_0^2 \right) = \frac{\tilde{\sigma}}{\ell_4} \quad (2.43)$$

Ignoring the anomalous correction, this gives the same form for y_0 as in (2.39). With this, the redshift factor between the DW and the bounce is found to be

$$\frac{R_0}{R_b} \simeq \frac{1}{(1 - \tilde{\sigma}^2)^{1/4}}.$$

Note that in order to obtain these planar solutions, what we are doing is to tune the DW tension against Λ_4 plus the Casimir term.

Yet, this does not make the solution self-consistent. For this, we still have to solve eq. (2.29). The function $\Delta\eta_*$ can be easily obtained explicitly in this case,

$$\Delta\eta_*(p_*) = \frac{h(\tilde{\sigma})}{(-\epsilon p_*/4)^{1/4}} \quad (2.44)$$

where

$$h(\tilde{\sigma}) = (1 + \text{sign } \tilde{\sigma}) \frac{2\sqrt{\pi} \Gamma(\frac{5}{4})}{\Gamma(\frac{3}{4})} - \frac{1}{2} \text{sign } \tilde{\sigma} B_{(1-\tilde{\sigma}^2)}\left(\frac{1}{4}, \frac{1}{2}\right) \quad (2.45)$$

with $B_z(a, b)$ the incomplete Beta function. Note that $h(\tilde{\sigma})$ vanishes for $\tilde{\sigma} \rightarrow -1$, as it should since in this limit the DW chops off all of the space.

Next, we need the form of $p(\Delta\eta)$ at, say, one loop for the planar walls. With the same kind of Karch-Randall boundary conditions, this boils down to computing the Casimir energy on $S_1 \times R^3$. Because there is no other scale in the problem, $p(\Delta\theta)$ can only be of

the form $\Delta\theta^{-4}$, where $\Delta\theta = \Delta\eta + \Delta\eta'$ is the length of the circle. Since the result must match the $S_1 \times AdS_3$ case for $\Delta\theta \rightarrow 0$, it can only be

$$p_{\text{KR}}^{1-loop} = -\frac{1}{3} \left(\frac{2\pi}{\Delta\eta + \Delta\eta'} \right)^4 \tag{2.46}$$

where as before, $\Delta\eta'$ is the conformal interval in the ‘adjacent’ CFT’ and so is a constant that parameterizes the boundary conditions. Note that it is not so clear that $\Delta\eta' = \pi$ is the natural value now, because that does not give global AdS_4 as the space where the CFT’ is defined anyway. In the following, we shall assume a generic value for $\Delta\eta'$.

The strong coupling result differs from (2.46) by a factor $3/4$ (see section 3.1.1). Of course, this is the same factor that appears in the usual AdS/CFT computations of the CFT at finite temperature [63, 57]. Hence, eq. (2.29) reads

$$\Delta\eta = h(\tilde{\sigma}) \left(\frac{4a(\lambda)}{\epsilon} \right)^{1/4} \frac{\Delta\eta + \Delta\eta'}{2\pi}$$

where at weak and strong coupling we have $a(0) = 3$ and $a(\infty) = 4$ respectively. Hence, we can express the conformal interval directly in terms of the DW tension, the ‘t Hooft coupling, the backreaction parameter ϵ and the boundary conditions ($\Delta\eta'$) as

$$\Delta\eta = \Delta\eta' \left[\frac{2\pi}{h(\tilde{\sigma})} \left(\frac{\epsilon}{4a(\lambda)} \right)^{1/4} - 1 \right]^{-1}, \tag{2.47}$$

and the Casimir energy as

$$p_{\text{KR}}^{1-loop} = -\frac{1}{a(\lambda)} \left(\frac{2\pi}{\Delta\eta'} \right)^4 \left[1 - \frac{h(\tilde{\sigma})}{2\pi} \left(\frac{4a(\lambda)}{\epsilon} \right)^{1/4} \right]^4 \tag{2.48}$$

Thus, from (2.47) we see that self consistent solutions exist whenever $\Delta\eta' \neq 0$, and $h(\tilde{\sigma})$ is small enough, that is, when the tension is close enough to $-\sigma_c$, the critical value given in (2.5). For every given $\epsilon \ll 1$, the planar DW solution with maximal tension $\sigma_{\text{max}}^{\text{planar}}$ is the one for which

$$h(\tilde{\sigma}_{\text{max}}^{\text{planar}}) = 2\pi \left(\frac{\epsilon}{4a(\lambda)} \right)^{1/4}.$$

We plot how $\sigma_{\text{max}}^{\text{planar}}$ depends on ϵ in figure 6. Note that, as mentioned above, these solutions cease to exist in the $\epsilon \rightarrow 0$ limit (only the $\sigma = -\sigma_c$ solution would survive in this limit). For small but finite ϵ , though, there is a finite range of the DW tension for which the solutions are trustable. Naturally, this range starts up at $-\sigma_c$ because this is when $\Delta\eta$ vanishes and hence p is maximal. As figure 6 shows, for moderately small $\epsilon \gtrsim 1/2$ one can have planar solutions with positive DW tension. Needless to say, at this point it is hard to tell whether these solutions are not present in the underlying theory or whether they are but with relative large corrections.

It is also worth pointing out that in principle there are solutions with no DWs ($\sigma = 0$) but still with some nontrivial Casimir effect, which is entirely supported by the slightly

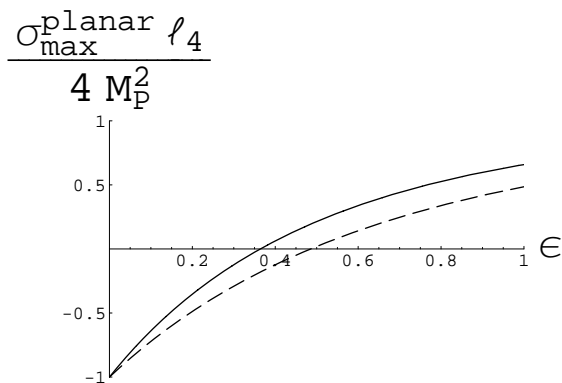


Figure 6: The planar Bootstrap DW solutions in the DW tension *vs* ϵ diagram fall in the area below the curves (KR-like boundary conditions are assumed). The solid and dashed lines correspond to weak ($\lambda \rightarrow 0$) and strong ($\lambda \rightarrow \infty$) coupling results respectively. Even for small ϵ , there are solutions for a finite range of tensions close to the critical value $-\sigma_c$ (see (2.5)). The maximal tension $\sigma_{\max}^{\text{planar}}$ is smaller at strong coupling. Hence, one can say that strong coupling effects in the CFT remove some of these quantum solutions.

unconventional choice of boundary conditions, of course. These arise for ϵ larger than

$$\epsilon_c = \frac{4a(\lambda)}{\pi^2} \left(\frac{\Gamma(5/4)}{\Gamma(3/4)} \right)^4$$

which is approximately 0.36 (0.48) for weak (strong) coupling. Hence, above this critical value new solutions of the gravity + CFT system with this kind of asymptotic behaviour open up.

Finally, let us briefly mention what happens for reflecting boundary conditions. In this case,

$$p_{\text{refl}}^{1\text{-loop}} = -\frac{1}{3} \left(\frac{\pi}{\Delta\eta} \right)^4 \tag{2.49}$$

and eq. (2.29) directly gives a $\Delta\eta$ -independent equation that links the DW tension with ϵ as

$$h(\tilde{\sigma}_{\text{refl}}^{\text{planar}}) = \pi \left(\frac{\epsilon}{4a(\lambda)} \right)^{1/4} .$$

Inverting this, one finds that the critical value of the tension that gives a planar solution is very close to $-\sigma_c$ for any $\epsilon < 1$. Note, that both $\Delta\eta$ and p are arbitrary for this solutions. This degeneracy is expected to disappear in the next order in ϵ .

3. 5D gravity dual

In this section, we discuss the 5D duals of the quantum corrected DW solutions presented in section 2. As before, we shall first consider the gravity dual ignoring the backreaction on the 4D metric, in section 3.1. This is the ‘standard’ version of the AdS/CFT correspondence, and boils down to finding the regular vacuum AdS_5 solutions (with no branes) with a

boundary metric conformal to the Domain Wall background. We then holographically include dynamical 4D gravity in section 3.2 by constructing the solutions where a DW localized on a Karch-Randall brane.

3.1 Ignoring the backreaction (the brane)

In section 2 we considered the maximally symmetric configurations, where the DW world-volume geometry is M_κ , i.e., a 2+1 dimensional de Sitter ($\kappa = 1$), Minkowski ($\kappa = 0$) or Anti de Sitter space ($\kappa = -1$). Hence, we only need to find asymptotically AdS_5 solutions with the same symmetries. A generalization of the Birkhoff theorem guarantees that the most general Λ -vacuum solution with these symmetries can be written locally as

$$ds_5^2 = \ell_5^2 f(R) d\theta^2 + \frac{dR^2}{f(R)} + R^2 ds_\kappa^2, \tag{3.1}$$

$$f(R) = \kappa + \frac{R^2}{\ell_5^2} + \frac{\mu}{R^2}$$

where $\ell_5^2 = -6M^3/\Lambda_5$ is the AdS_5 curvature radius, $M = (8\pi G_5)^{-1/3}$ is the bulk Planck mass and μ is an integration constant proportional to the Weyl curvature of the solution. As before, ds_κ^2 is the line element on M_κ with unit radius. The $\kappa = 1$ case includes the (higher dimensional generalization of the) BTZ black hole and the Schwarzschild-AdS bubble of nothing solutions. For $\kappa = 0$ and $\mu \neq 0$ (3.1) is the AdS-Soliton. Here we shall be most interested in the $\kappa = -1$ case. For $\mu = 0$, it gives global AdS_5 and for $\mu \neq 0$ it is what we will call a ‘hyperbolic AdS Soliton’.

We shall be most interested in the ‘non-extremal’ cases, for which $f(R)$ has simple zeroes. Then, the larger root of $f(R)$ is

$$R_+ = \frac{\ell}{\sqrt{2}} \left(-\kappa + \sqrt{\kappa^2 - 4\mu/\ell_5^2} \right)^{1/2} \tag{3.2}$$

Hence, R ranges from R_+ to ∞ and R_+ represents the center of the axial symmetry (which is present in the absence of the brane and the DW). In order not to have a conical singularity at $R = R_+$, one has to periodically identify θ with period

$$\Delta\theta = \frac{4\pi}{\ell_5 f'(R_+)} = 2\pi \left(\frac{-\kappa + \sqrt{\kappa^2 - 4\mu/\ell_5^2}}{2(\kappa^2 - 4\mu/\ell_5^2)} \right)^{1/2}. \tag{3.3}$$

Hence, in all these cases, the coordinate θ is periodic, and the boundary is conformal to $S_1 \times M_\kappa$. According to the AdS/CFT correspondence, these solutions can be matched to the states of $\mathcal{N} = 4$ SYM on the boundary at strong coupling. Let us now use this correspondence to infer the stress tensor of the CFT at strong coupling for the case of our interest.

3.1.1 Casimir energy on $AdS_3 \times S_1$ at strong coupling

For the AdS_3 slicing, the 5D metric corresponds to the Hyperbolic AdS Solitons, i.e., eq. (3.1) with $\kappa = -1$. In order that these solutions are regular, the integration constant must obey $\mu < \ell_5^2/4$.

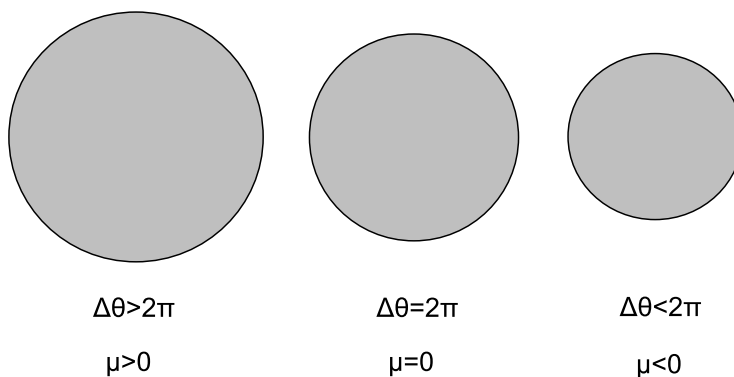


Figure 7: Hyperbolic AdS solitons with different ‘radii’ $\Delta\theta$ can be represented as disks of different sizes. Every point represents an AdS_3 with a curvature radius given by (3.2) at the origin while at infinity it grows as fast as the circle spanned by θ . The boundary is of the form $S_1 \times AdS_3$, and the length of the S_1 in units of the AdS_3 radius is $\Delta\theta$, (3.3). Global AdS_5 is the particular case $\mu = 0$.

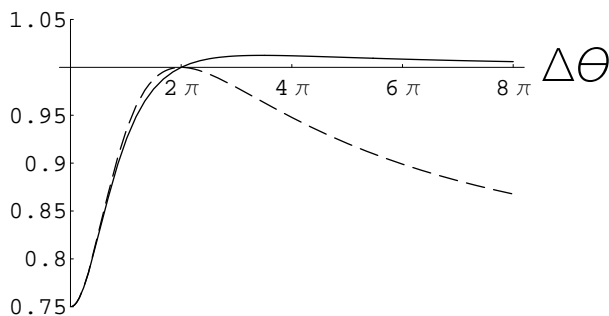


Figure 8: Comparison between the weak and strong coupling forms of the Casimir Energy on $S_1 \times AdS_3$ with antiperiodic boundary conditions for the fermions. The solid and dashed lines are p^{NP}/p^{1-loop} and $\langle T_0^0 \rangle^{NP}/\langle T_0^0 \rangle^{1-loop}$ respectively. For a single DW and KR boundary conditions $\Delta\theta$ ranges from π to 3π , while for reflecting boundary conditions $0 < \Delta\theta < 4\pi$.

The structure of these spacetimes is very similar to global AdS. To visualize it, it is convenient to suppress the AdS_3 factors. The geometry spanned by the R and θ ‘polar’ coordinates is a hyperboloid, with the topology of a disk. The boundary of the disk has infinite volume, but we can always make a conformal transformation to bring it to a finite size. Then, the difference between these spaces (3.1) with different values of μ is that the length of this disk is different,⁹ as shown in figure 7.

The important point is that the boundary of these geometries is of the form $AdS_3 \times S_1$ with different S_1 lengths. In section 2.2.2, we computed the 1-loop Casimir energy of the CFT on this geometry. Now, using the AdS/CFT correspondence, it is straightforward to obtain the non-perturbative form of the Casimir energy for large ‘t Hooft coupling to

⁹The Hyperbolic AdS Solitons can actually be viewed as purely gravitational Cosmic Strings (codimension 2 objects). We comment on this in section 4.

leading order in the $1/N$ expansion. According to the correspondence, this is given by the energy of the 5D gravity solution (3.1). Since the metric (3.1) is asymptotically AdS_5 , one can use the prescription introduced in [64]. Upon rescaling the boundary metric so that it coincides with (2.13), and expressing the 5D quantities directly in terms of the CFT ($\ell_5^2 M^3 = N^2/4\pi$), one obtains [65]

$$\langle T_{\mu}^{\nu} \rangle^{\text{NP}} = \frac{3N^2}{32\pi^2} \frac{1}{R_*^4} \left(1 - \frac{4\mu}{\ell_5^2} \right) \text{diag} \left(-\frac{1}{3}, -\frac{1}{3}, -\frac{1}{3}, 1 \right)_{\mu}^{\nu}. \quad (3.4)$$

The first piece in the parenthesis is readily identified as the anomaly term. Thus, the second term is the non-perturbative form of the Casimir energy, that is, $p^{\text{NP}} = 4\mu/\ell_5^2$. Expressing μ in terms of $\Delta\theta$ by means of (3.3), one obtains

$$p^{\text{NP}}(\Delta\theta) = 1 - \frac{2\pi^2}{\Delta\theta^2} - 2\pi^4 \frac{1 + \sqrt{1 + 2\Delta\theta^2/\pi^2}}{\Delta\theta^4}. \quad (3.5)$$

This expression can be directly compared to the weak coupling result (2.23). As shown in figure 8, the difference between the weak and strong coupling Casimir energies is quite modest. The maximum discrepancy is for $\Delta\theta \rightarrow 0$, for which one has the famous $3/4$ suppression at strong coupling. It is noteworthy that for $\Delta\theta > 2\pi$ the Casimir Energy at strong coupling is actually *larger* than at weak coupling, with a maximum enhancement by a factor $81/80$. Instead, the full stress tensor (including the anomaly term) is always smaller for any $\Delta\theta$. Notice as well that p^{NP} again vanishes for $\Delta\theta = 2\pi$ (pure AdS_4), as it should because $\mu = 0$ is an exact string state.

Since, argued above, the Casimir energy can also be viewed as the amount of particles produced by the accelerating DW, we conclude that for this system strong coupling effects do not dramatically suppress the particle production. As we shall see in section 3.2 (together with the results of section 2.3), the inclusion of the backreaction does not change this conclusion.

3.2 Localized Domain Walls in the Karch-Randall model

Let us finally turn to the actual dual of the setup described in section 2, the Karch-Randall model [18]. The 4D quantum corrected Domain Wall solutions simply correspond to the solutions representing a Domain Wall localized on the brane (from now on, by ‘the brane’ we will mean the 3+1 brane, not the DW). In the Karch-Randall model, the brane tension τ is set below the critical or ‘Randall-Sundrum’ value $\tau_{\text{RS}} = 6M^3/\ell_5$ so that its geometry is (asymptotically) AdS_4 .

In the next derivation, we will follow refs. [66, 29, 60]. As before, we will concentrate on the solutions with the symmetries of a maximally symmetric DW, that is with a 3D maximally symmetric slicing. The (double-Wick rotated version of the) Birkhoff theorem guarantees that the most generic solution with this symmetry can be written locally as (3.1). In terms of these ‘bulk adapted’ coordinates, the full spacetime can be constructed as usual by finding the embedding of the brane in the bulk, cutting the bulk along the brane and gluing two copies by the brane location (we are assuming Z_2 symmetry across the brane).

With the assumed symmetry, the location of the brane can be parameterized by two functions $(R(y), \theta(y))$, and solve for them by imposing that the Israel junction conditions are satisfied. A level of arbitrariness is still present, due to the re-parametrization (gauge) invariance of the embedding. To fix the gauge, it is convenient to choose

$$\ell_5^2 f(R) \theta'^2 + \frac{R'^2}{f(R)} = 1. \tag{3.6}$$

With this condition, the induced metric on the brane precisely takes the form (2.2), and y is the proper distance on the brane orthogonal to the DW. Also, once $R(y)$ is known then one can solve for $\theta(y)$ by integrating eq. (3.6) and the full solution will be determined.

As is well known, the Israel junction conditions for the brane lead to a ‘Friedman’ equation

$$\frac{R'^2 - \kappa}{R^2} = \left(1 - \frac{\epsilon}{4}\right) \frac{1}{\ell_4^2} + \frac{\mu}{R^4}, \tag{3.7}$$

where now

$$\frac{1}{\ell_4^2} = -\frac{\delta\tau}{3M_P^2}$$

(as before, $\epsilon \equiv \ell_5^2/\ell_4^2$) and we used $M^3\ell_5 = M_P^2$.

Obviously, (3.7) is almost identical to the four dimensional counterpart of the Friedman equation, (2.25) once we identify the Casimir term as

$$\mu = \frac{\ell_5^2}{4} p. \tag{3.8}$$

To be precise, the brane-world version of the Friedman equation is equivalent only to the leading order in the backreaction parameter ϵ , since to leading order the anomaly term in (2.25) is just the constant $-\epsilon/(4\ell_4^2)$. It immediately follows that the correspondence between the brane-world setup (may it be the Randall-Sundrum or the Karch-Randall model) and the 4D gravity + strongly coupled CFT system holds to the leading order in the backreaction.

As in section 2, the Friedmann equation (3.7) holds away from the DW location, and in order to take this into account one needs an appropriate matching condition. As worked out in [29], this reads

$$\frac{1}{\ell_5} \arctan\left(\frac{K_0 \ell_5}{1 - \epsilon/2}\right) = \frac{\sigma}{4M_P^2}, \tag{3.9}$$

where $K_0 \equiv -(R'/R)|_{0+}$, as before. This junction condition is equivalent to (2.27) up to order ϵ , as expected because the leading correction in (2.27) arises from the trace anomaly [29].

So far, we see that solving the R part of the embedding is (almost) equivalent to finding the warp factor for the quantum corrected 4D DWs. Let us see now what we obtain when we work out $\theta(y)$. From (3.6) and (3.7), one arrives at

$$\theta' = \left(1 - \frac{\epsilon}{2}\right) \frac{R}{\ell_5^2 f(R)}$$

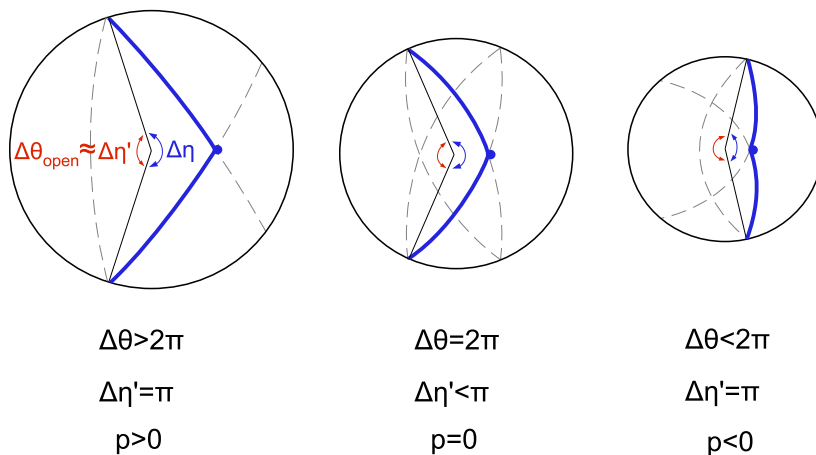


Figure 9: Schematic view of the localized Domain Walls in the one brane case (corresponding to KR boundary conditions). The blue solid line represents the 3+1 brane and the DW is the blue dot. The bulk corresponds to two copies of the left side of the brane glued together. The dashed gray lines represent the continuation of the brane embedding in the absence of the DW and are meant to indicate how to construct the solutions. The center diagram shows the locally AdS solution, for which there is no radiation ($p = 0$). For positive DW tension, the brane sweeps more than half of the disk and the remaining opening angle $\Delta\theta_{\text{opening}} \simeq \Delta\eta'$ is less than π . Hence, this solution is not asymptotically global AdS₅. The left (right) diagram corresponds to a solution with a positive (negative) tension DW and asymptotically global AdS₅ boundary condition. Again, the opening angle is less (more) than half of the original disk. But given that the length of the S_1 — the boundary of the disk — can differ from 2π , one can have asymptotically global AdS if the S_1 is larger (smaller) than 2π . For this to happen, the Weyl curvature μ — and hence the Casimir Energy p — must be positive (negative).

This means that the angle $\Delta\theta_{\text{brane}}$ swept by the brane from $y \rightarrow -\infty$ to $+\infty$ is

$$\Delta\theta_{\text{brane}} = \int_{-\infty}^{\infty} \theta' dy = 2 \left(1 - \frac{\epsilon}{2}\right) \left[\int_{R_b}^{\infty} + \text{sign}\sigma \int_{R_b}^{R_0} \right] \frac{R}{\ell_5^2 f(R)} \frac{dR}{R'(R)} \quad (3.10)$$

where again R_b denotes the bounce in the warp factor and $R'(R)$ is found from (3.7). Note that to leading order in ϵ , this precisely coincides with the conformal interval of the 4D geometry, eq. (2.28). Hence, we see that the angle θ is an approximate measure of the conformal coordinate. This gives a geometric justification to the identification of the length of the S_1 as (2.14) in terms of the conformal intervals for the CFT and the CFT' that we argued for in section 2.

Furthermore, it becomes very clear how to impose the boundary conditions in terms of $\Delta\theta_{\text{brane}}$. As mentioned earlier, the bulk consists of two copies of the space (3.1) cut along the brane trajectory. Picturing these spaces as disks as in figure 7, the brane is going to remove a certain wedge-like shape from the disk. Now, if one is to impose that the 5D metric away from the brane is asymptotically *global* AdS₅, then the total opening angle left out by the brane should be π . In equations, what we have in general is

$$\Delta\theta_{\text{opening}} = \Delta\theta - \Delta\theta_{\text{brane}}, \quad (3.11)$$

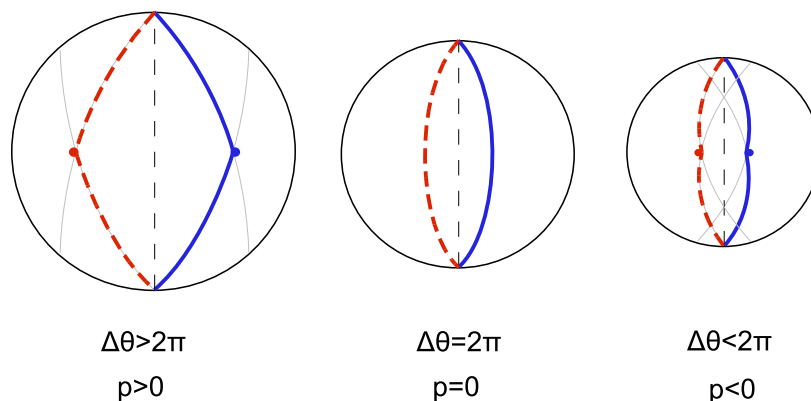


Figure 10: Schematic view of the localized Domain Walls in the two brane KR model (corresponding to reflecting boundary conditions). The straight dashed line indicates the ‘equator’ across which the Z_2 symmetry is imposed. The solid-blue and dashed-red lines represent each brane, and the dots the corresponding localized DWs. The left, right and central diagrams correspond to positive, negative and zero tension DWs respectively.

where $\Delta\theta$ is given by (3.3) in order to avoid a conical singularity in the bulk. The boundary condition corresponding to asymptotically global AdS_5 corresponds to setting $\Delta\theta_{\text{opening}} = \pi$. Since $\Delta\theta$ is a function only of μ (that is, the Casimir energy) and $\Delta\theta_{\text{brane}}$ also depends on the DW tension σ (as well as on ℓ_4), this gives a relation between μ and σ , which is going to agree with that of section 2 to leading order in ϵ , of course.

In fact, it is slightly more illuminating to rewrite (3.11) as

$$\Delta\theta = \Delta\theta_{\text{brane}} + \Delta\theta_{\text{opening}} .$$

This is the counterpart of eq. (2.30). We identify $\Delta\theta(\mu)$ as the strongly coupled version of $\Delta\theta^{1-loop}(p)$, $\Delta\theta_{\text{brane}}$ with the conformal interval $\Delta\eta$, and $\Delta\theta_{\text{opening}}$ with $\Delta\eta'$. This clearly shows the relation between the choice of the boundary condition in the AdS_5 bulk and the boundary condition for the CFT'.

Hence, the dual of the logic that let us conclude in section 2 that subcritical DWs radiate particles is the following. In the presence of a DW, the brane sweeps an angle $\Delta\theta_{\text{brane}}$ that is more than half of disk corresponding to pure AdS_5 . In order that the remaining opening angle stays equal to π , the only option is that the disk is actually larger than 2π . This demands that the μ (and hence the Casimir Energy) is nonzero.

In figure 9, we represent schematically how these localized DW solutions look like. We include for comparison the case when the bulk is asymptotically global AdS_5 and the case when it is locally AdS_5 . In these diagrams, we also depict the embedding of another ‘fake’ brane with the same tension at the ‘opposite side’ of the bulk would take. One can think that the CFT' is defined on that brane. For the global AdS boundary condition, the geometry on the fake brane is conformal to pure AdS_4 (its conformal interval is $\Delta\eta' = \pi$), while for the locally AdS_5 condition, it has a DW' with tension $-\sigma$.

Let us now comment on the reflecting boundary conditions. These are implemented by imposing another Z_2 symmetry across the ‘equator’ of the bulk. In particular this

demands the presence of a second identical brane with an identical DW on it. Hence, in this case one has

$$\Delta\theta_{\text{brane}} = \frac{\Delta\theta}{2},$$

which is the dual of (2.17). The corresponding solutions are depicted in figure 10.

Finally, we should refer to what are the duals of the ‘Bootstrap’ Domain Wall spacetimes. As explained in section 2.3.2, in the 4D picture when one includes the backreaction from the Casimir energy, there are DW solutions with with subcritical tension (*i.e.*, with tension smaller than σ_c as given by (2.5)) that are planar or even inflating. The curvature scale of these solutions is well below the cutoff everywhere, so they can be trusted. Since the KR model is a UV completion of the 4D gravity + CFT system, analogous solutions should be present, and indeed they are.

The duals of the Bootstrap DW solutions simply are localized DW solutions like those depicted in figures 9 and 10, but where one picks the $\kappa = 1$ or $\kappa = 0$ slicing of the bulk, for either inflating or planar DWs respectively. Since, as already emphasized, the angular coordinate θ in the bulk coincides with the conformal coordinate to leading order in ϵ , the analysis done in section 2.3.2 already guarantees that for small ϵ there exist localized planar or inflating DW solutions with subcritical tension (one expects a similar behaviour for inflating DWs). As we have seen in section 2.3.2, these solutions exist when the DW tension is comprised between $-\sigma_c$ and an ϵ -dependent maximal value $\sigma_{\text{planar}}^{\text{max}}(\epsilon)$, see figure 6. In the 5D gravity dual, $\sigma_{\text{planar}}^{\text{max}}(\epsilon)$ differs from that obtained in the CFT picture for two reasons: first, because of the large ‘t Hooft coupling and second, because the dependence on the ‘backreaction parameter’ ϵ only coincides for $\epsilon \ll 1$. In particular, one can imagine that for moderately small values of ϵ the duals of the Bootstrap DW solutions ‘disappear’. The large ‘t Hooft coupling can be easily accounted for by taking the form of $p(\Delta\theta)$ at strong coupling, as has already been done in section 2.3.2 in the planar case. As shown in figure 6, the range of DW tensions leading to Bootstrap solutions is smaller. Hence, in a sense, one can say that strong coupling effects ‘remove’ some of the solutions where the quantum effects are important. However, this seems a bit marginal effect.

On the other hand, to see whether these solutions disappear for larger values of ϵ , one should obtain $\sigma_{\text{planar}}^{\text{max}}(\epsilon)$ by solving (3.11) rather than (2.30). A more detailed study is deferred for the future, but preliminary results indicate that for modelately small ϵ the picture suggested by figure 6 is not significantly changed.

4. Epilogue: cosmic strings in AdS

Let us finally discuss the gravitational field created by a Cosmic Strings, that is a relativistic (pure tension) codimension 2 brane, in asymptotically AdS space. This apparently unrelated issue will turn out to give quite interesting insight. The following discussion can be done in arbitrary number of dimensions $D \geq 4$, but for the sake of simplicity we shall restrict to the 5D case, in which the Cosmic Strings worldsheet is 2+1 dimensional.

As is well known, it is very easy to obtain the gravitational effect of a CS in any ambient spacetime in the thin wall approximation as long as one has a symmetry axis [67].

The usual prescription is to cut a wedge, which can simply be done by reducing the range of the angular polar coordinate. For example, for AdS in Poincaré coordinates

$$\frac{\ell_5^2}{w^2} [dw^2 - dt^2 + dz^2 + d\rho^2 + \rho^2 d\phi^2] , \tag{4.1}$$

if the range of the angle is $0 < \phi < 2\pi - \delta$ then this is the metric for a CS with tension $\sigma = M^3\delta$. It is also obvious that locally this metric is isometric to pure AdS, and it only differs from it globally. It follows that for the solution (4.1) the Newtonian potential vanishes and so the CS exerts no attraction/repulsion on test particles. Moreover, the Weyl curvature also vanishes identically everywhere (except at the location of the string, of course), and so there are no tidal forces either.

However, we shall now argue that (4.1) does *not* represent the actual gravitational field produced by a CS in AdS. The reason is that the boundary conditions for such an object in AdS are not unique, and as we shall see, those implicitly assumed to obtain (4.1) are not the most natural ones. Indeed, far away from the CS, the metric (4.1) does not approach global AdS. However, it is very easy to explicitly construct another CS solution that is asymptotically global AdS and which enjoys the same symmetries. This is simply given by one of the hyperbolic AdS solitons (3.1) (with $\kappa = -1$) with a wedge removed. As we have seen in the previous section, once $\mu \neq 0$, the length of the S_1 factor $\Delta\theta$ must be given by (3.3) in the hyperbolic AdS soliton if one is to avoid a conical singularity at the center. But that is precisely what we want for a CS solution. Hence, by choosing $\Delta\theta$ differently from (3.3), we will obtain one such CS solution. For an asymptotically globally AdS CS solution, we only need to choose $\Delta\theta = 2\pi$ (with $\mu \neq 0$). Equivalently, one can think that we are removing a wedge from a regular AdS Hyperboloid, in such a way that the length of S_1 equal to 2π and at the same time have a CS at the origin ($R = R_+$). The resulting ‘witch-hat’¹⁰ geometry is essentially the same as the Hyperbolic AdS soliton but with a conical tip at the center.

Note that the reason why it is possible to find CS solutions that do not affect the asymptotic structure of the spacetime in AdS is that the Hyperbolic AdS soliton itself can be viewed as a regular pure gravity cosmic string-like solution, that is a codimension 2 lump of (Weyl) curvature. The deficit angle produced by the ‘material’ Cosmic String can thus be compensated by that produced by the AdS soliton. The Weyl curvature, of course is not compensated for and this is the effects that remains at infinity.

Now that we know the asymptotically globally AdS CS metrics, let us describe its properties. With the inclusion of the CS, the relation between the range of the angular coordinate $\Delta\theta$, the integration constant μ and the CS tension is

$$\frac{\ell_5 f'(R_+)}{2} \Delta\theta = \left(2\pi - \frac{\sigma}{M^3} \right) .$$

The metric (4.1) corresponds to (3.1) with $\mu = 0$ (and hence $\Delta\theta = 2\pi - \sigma/M^3$), written in more common coordinates. For the asymptotically globally AdS metric, instead, $\Delta\theta = 2\pi$

¹⁰We thank Lorenzo Sorbo for suggesting this term to us.

and the Weyl curvature is given in terms of the CS tension as

$$\mu = \frac{\ell_5^2}{32} \left(8 - 4(1 - \hat{\sigma})^2 - (1 - \hat{\sigma})^4 - (1 - \hat{\sigma})^3 \sqrt{8 + (1 - \hat{\sigma})^2} \right) \quad (4.2)$$

where $\hat{\sigma} \equiv \sigma/(2\pi M^3)$. Note that when the deficit angle becomes close to 2π ($\hat{\sigma} = 1$), μ approaches the extremal value $\mu = 4\ell_5^2$, for which the metric develops an infinitely long throat. This is nothing but expected, because in this case the geometry close to the string should be close to a thin cylinder.

The magnitude of the Weyl curvature $|W^{\mu\nu\rho\sigma}W_{\mu\nu\rho\sigma}|^{1/2}$ is of order μ/R^4 . Hence, it is clear that in this solution the CS produces long range Weyl curvature and hence tidal forces. Notice that tidal forces can be produced by wiggling or moving CSs (as well as by non-relativistic ones). The surprising thing here is that they are produced in a static, ‘straight’ (maximally symmetric) configuration. Hence, we should ascribe this as a real gravitational effect of the strings. The scale of the tidal forces close to the CS location is of order

$$\frac{\mu}{R_+^4} \sim \frac{1}{\ell_5^2} \frac{\sigma}{M^3}$$

for small σ . Hence, this effect is sensitive to the curvature scale produced by ‘the other’ sources (in this case, the cosmological constant), which is why we do not have it for $\Lambda = 0$.¹¹

Let us now show that in these solutions the CS generates a nontrivial Newtonian potential that translates into a repulsive force on test particles. A quick way to see this is by writing the metric (3.1) in the Schwarzschild-like coordinates

$$ds_5^2 = \ell_5^2 f[R(r)] d\theta^2 + \frac{dr^2}{g(r)} + g(r) ds_{AdS_3}^2 . \quad (4.3)$$

Taking the AdS_3 slices in global coordinates, $-(1+(x/R_+)^2)dt^2 + dx^2/(1+(x/R_+)^2) + x^2 d\phi^2$, the Newtonian potential is simply given by

$$2\phi_N = g(r)(1 + (x/R_+)^2) - 1 .$$

Comparing (4.3) to (3.1), one sees that $g(r) = R^2(r)/R_+^2$ and

$$r(R) = \int_{R_+}^R \frac{R' dR'}{\ell_5 \sqrt{f(R')}} , \quad (4.4)$$

which can be written explicitly in terms of Elliptic functions. For our purposes, though, it will suffice to know the form of $r(R)$ for small and large r . At large distances, one finds

$$r \simeq R + c + O(R^{-1})$$

¹¹It is possible to construct solutions with Weyl curvature (and maximal symmetry) with $\Lambda > 0$. However, it is not clear that these are relevant at all as happens for $\Lambda < 0$, because the asymptotic structure of the resulting spacetime always differs from de Sitter. It would be interesting to understand under what circumstances the CS can generate nontrivial gravitational effects as those presented here. A more thorough analysis will be left for the future.

where c is a μ dependent constant. It is easy to show that for small μ ,

$$c \simeq \frac{\pi \mu}{4 \ell_5^2} .$$

From this, one immediately finds that

$$g(r) = \frac{r^2 - 2cr}{\ell_5^2} (1 + O(\mu/\ell^2)) + \dots ,$$

where the dots indicate subleading terms in $1/r$. Hence, at linear level in the CS tension, the Newtonian potential develops a linear component far away from the CS, corresponding to a constant gravitational repulsion (for $\sigma > 0$) given by

$$\frac{\pi \sigma}{4 M^3 \ell_5} .$$

It is perhaps surprising to find that a positive tension CS induces a repulsive force. Intuitively, the reason for this seems to be that in order to cancel the deficit angle at infinity we have to start with an AdS soliton with opposite tension, and this is what really gives the Newtonian potential.

On the other hand, for small r , one has $r^2 \simeq (R^2 - R_+^2)/(1 - (R_-/R_+)^2) + \dots$, where R_{\pm} are the two roots of $f(R) = 0$ and the dots indicate higher powers of $R^2 - R_+^2$. Hence,

$$\frac{g(r)}{g(0)} = \frac{R^2}{R_+^2} = 1 + b^2 r^2 + \dots \quad \text{with} \quad b^2 = \frac{R_+^2 - R_-^2}{R_+^4} .$$

Hence, the Newtonian potential is quadratic as usual in AdS. Furthermore, for small μ one has

$$b^2 \simeq \frac{1}{\ell_5^2} - \frac{\mu^2}{\ell_5^4} + \dots$$

so, at linear level in the CS tension, the Newtonian potential close to the CS precisely coincides with that of the usual locally AdS solution. This is nothing but expected, since in this region the geometry is approximately conical, and this already accounts for the gravitational effect of the CS at linear level.

In summary, the picture is that for a CS with small tension, close enough to the CS everything looks ‘normal’, i.e., it generates no Newtonian potential, the Weyl curvature is essentially irrelevant and all the gravitational effects arise because the geometry is locally conical. However, after a certain distance, the Weyl curvature starts to become important, the notion of the conical-type space is lost and the deficit angle is replaced by a gravitational repulsion. Naturally, the scale where the change of regime occurs is given by the curvature radius associated to the Weyl curvature, which for small σ is

$$\frac{\ell_5}{\sqrt{|\sigma|/M^3}} .$$

It is impossible not to notice the quite striking similarity between this and the screening effect that one would expect in a massive gravity theory, even though here we have only

assumed ordinary gravity in AdS. Of course, the details of a really massive gravity theory like AdS plus a CFT with KR boundary conditions are different, but we already see that even without the CFT there are some elements in common. Indeed, in a sense, the deficit angle at infinity is completely ‘screened away’, and instead, a new kind of behaviour appears at large distances. Furthermore, such a change of behaviour only appears because we are insisting in having a certain kind of boundary condition — asymptotically global AdS. It is unclear to us whether there is any deep reason why the gravitational effect of a CS in AdS should display this massive-like fashion, but it might be that it is a peculiarity of codimension-2 sources only.

So far, we have seen that aside from the ordinary locally AdS CS solutions, there is another one with the same symmetries that is asymptotically global AdS, with rather different properties. From a physical point of view, then, we should ask from which solution should we extract the actual gravitational behaviour of the CS in AdS, or in other words, what boundary condition should one impose? Of course this choice is context-dependent, but still in a generic case one should be able to specify what is the most natural choice.

For this purpose, it seems quite clear to us that the asymptotically globally AdS should be preferred. Generically, whenever one finds several solutions for the same given source, and one of them shares the same asymptotic structure as the background, then this seems preferred. In terms of the linearized theory around that background, presumably this means that for this solution the metric perturbation is normalizable. In principle, it may well be (as happens with the CS in asymptotically flat space) that there is no normalizable solution. In that case, there is no alternative and the CS will change the global structure at infinity. But in AdS this does not need to be so: the persistence of the wedge at infinity can be traded by the presence of a long range Weyl curvature. From a physical point of view, one can always consider situations where the cosmic string is produced dynamically by some mechanism localized in some finite region. If initially the space is asymptotically global AdS, then once the CS is created one should still have the same asymptotics.

Finally, let us point out that the curvature scale on the string is $-1/R_+^2$ with R_+ given in (3.2), so this also depends on the string tension. Hence, one obtains a nontrivial ‘Friedmann equation’ (understood as the relation between the curvature scale and the tension or energy density on the defect; this is more relevant for the generalization of the present example to 6D, in which case the CS would be a 3+1 brane). In fact, the Friedmann equation would be quite peculiar, because the larger σ is, the more negative the curvature scale becomes. This is not so strange of course because one does not have lower dimensional gravity localized on the defect. However, this is illustrative as an extreme case where even with a noncompact bulk there is no self-tuning mechanism at work (once the asymptotically globally AdS boundary condition is enforced).

5. Conclusions

- A relativistic Domain Wall (DW) is a physical implementation of a uniformly accelerating mirror. In AdS_4 , whenever the DW acceleration exceeds the curvature scale $1/\ell_4$, there is no particle production into conformal fields in the maximally symmetric

configuration (both at weak and strong coupling). However, subcritical DWs (with acceleration $< 1/\ell_4$) generate a nontrivial CFT particle production that can be in equilibrium with the DW and the AdS_4 boundary.

- The amount of CFT radiation produced by subcritical DWs in AdS_4 is not dramatically sensitive to whether the CFT is weakly or strongly coupled (see figure 8). With Karch-Randall (KR) boundary conditions, the energy density in the radiation at weak and at strong coupling agree within a few %, and for reflecting boundary conditions the maximum discrepancy is a factor 3/4.
- The Karch-Randall type boundary conditions really represent a family of conditions. They encode the choice of boundary conditions for the CFT in the choice of vacuum for the ‘adjacent’ CFT’. The only natural choice is that the CFT’ is in the *ground state* in a space conformal to pure AdS_4 , which corresponds in the 5D dual to choosing an asymptotically *globally* AdS_5 bulk. Departing from this condition can lead to considerably different amount of radiation (both at weak and strong coupling), but this corresponds to a CFT in a quite exotic state.
- Once the boundary conditions between the two sides are appropriately matched, the DW solutions with the backreaction from the CFT included agree with the solutions for DWs localized on the brane in the Karch-Randall model to leading order in the backreaction. This confirms the holographic interpretation of the KR model as a CFT coupled to 4D (semiclassical) gravity in AdS_4 .
- We found a new type of solutions (the ‘Bootstrap’ DW spacetimes) which exist thanks to the backreaction from $\langle T_{\mu\nu} \rangle^{\text{CFT}}$ (for $\Lambda_4 < 0$). These solutions have no classical analog. Yet, they have a 5D gravity dual, further confirming the cutoff AdS/CFT correspondence.
- Our results also comply with the massive gravity interpretation of the Karch-Randall setup. The backreaction of the produced radiation leads to a screening of the DW tension, which depends on the boundary conditions. For KR boundary conditions there is more screening than for reflecting boundary conditions, as expected since the KR choice leads to a nonzero graviton mass.
- The phenomenon dual to the particle creation by subcritical DWs in AdS is that pure-tension codimension 2 branes in AdS are repulsive and produce long range Weyl curvature, i.e., tidal forces. This effect is quite interesting by itself, since this is rather different from the usual behaviour in flat space. It would be interesting to see whether it is peculiar to AdS or whether it also happens more generically whenever a codimension 2 brane is placed in an already curved space.

Acknowledgments

I thank JJ Blanco-Pillado, G Dvali, G Gabadadze, J Garriga, L Grisa, A Iglesias, M Kleban, M Porrati, M Redi and T Tanaka for useful discussions and R Emparan for

very valuable comments on a previous version of the paper. I also thank the organizers and participants of the “Quantum Black Holes, Braneworlds and Holography” workshop (Valencia, May 12-16 2008) for their feedback. This work has been partially supported by DURSI under grant 2005 BP-A 10131 and the David and Lucile Packard Foundation Fellowship for Science and Engineering

References

- [1] J.M. Maldacena, *The large- N limit of superconformal field theories and supergravity*, *Adv. Theor. Math. Phys.* **2** (1998) 231 [*Int. J. Theor. Phys.* **38** (1999) 1113] [[hep-th/9711200](#)].
- [2] E. Witten, *Anti-de Sitter space and holography*, *Adv. Theor. Math. Phys.* **2** (1998) 253 [[hep-th/9802150](#)].
- [3] S.S. Gubser, I.R. Klebanov and A.M. Polyakov, *Gauge theory correlators from non-critical string theory*, *Phys. Lett.* **B 428** (1998) 105 [[hep-th/9802109](#)].
- [4] H.L. Verlinde, *Holography and compactification*, *Nucl. Phys.* **B 580** (2000) 264 [[hep-th/9906182](#)].
- [5] S.S. Gubser, *AdS/CFT and gravity*, *Phys. Rev.* **D 63** (2001) 084017 [[hep-th/9912001](#)].
- [6] N. Arkani-Hamed, M. Porrati and L. Randall, *Holography and phenomenology*, *JHEP* **08** (2001) 017 [[hep-th/0012148](#)].
- [7] L. Randall and R. Sundrum, *An alternative to compactification*, *Phys. Rev. Lett.* **83** (1999) 4690 [[hep-th/9906064](#)].
- [8] R. Emparan, A. Fabbri and N. Kaloper, *Quantum black holes as holograms in AdS braneworlds*, *JHEP* **08** (2002) 043 [[hep-th/0206155](#)].
- [9] T. Tanaka, *Classical black hole evaporation in Randall-Sundrum infinite braneworld*, *Prog. Theor. Phys. Suppl.* **148** (2003) 307 [[gr-qc/0203082](#)].
- [10] A.L. Fitzpatrick, L. Randall and T. Wiseman, *On the existence and dynamics of braneworld black holes*, *JHEP* **11** (2006) 033 [[hep-th/0608208](#)].
- [11] A. Chamblin, S.W. Hawking and H.S. Reall, *Brane-World black holes*, *Phys. Rev.* **D 61** (2000) 065007 [[hep-th/9909205](#)].
- [12] L. Randall and R. Sundrum, *A large mass hierarchy from a small extra dimension*, *Phys. Rev. Lett.* **83** (1999) 3370 [[hep-ph/9905221](#)].
- [13] P.R. Anderson, R. Balbinot and A. Fabbri, *Cutoff AdS/CFT duality and the quest for braneworld black holes*, *Phys. Rev. Lett.* **94** (2005) 061301 [[hep-th/0410034](#)].
- [14] A. Fabbri and G.P. Procopio, *Quantum effects in black holes from the Schwarzschild black string?*, *Class. and Quant. Grav.* **24** (2007) 5371 [[arXiv:0704.3728](#)].
- [15] A. Fabbri, S. Farese, J. Navarro-Salas, G.J. Olmo and H. Sanchis-Alepuz, *Semiclassical zero-temperature corrections to Schwarzschild spacetime and holography*, *Phys. Rev.* **D 73** (2006) 104023 [[hep-th/0512167](#)].
- [16] T. Tanaka, *Implication of classical black hole evaporation conjecture to floating black holes*, [arXiv:0709.3674](#).

- [17] N. Tanahashi and T. Tanaka, *Time-symmetric initial data of large brane-localized black hole in RS-II model*, *JHEP* **03** (2008) 041 [[arXiv:0712.3799](#)].
- [18] A. Karch and L. Randall, *Locally localized gravity*, *JHEP* **05** (2001) 008 [[hep-th/0011156](#)].
- [19] M. Porrati, *Mass and gauge invariance. IV: holography for the Karch-Randall model*, *Phys. Rev.* **D 65** (2002) 044015 [[hep-th/0109017](#)].
- [20] R. Bousso and L. Randall, *Holographic domains of anti-de Sitter space*, *JHEP* **04** (2002) 057 [[hep-th/0112080](#)].
- [21] M. Porrati, *Higgs phenomenon for 4 – D gravity in anti de Sitter space*, *JHEP* **04** (2002) 058 [[hep-th/0112166](#)].
- [22] M.J. Duff, J.T. Liu and H. Sati, *Complementarity of the Maldacena and Karch-Randall pictures*, *Phys. Rev.* **D 69** (2004) 085012 [[hep-th/0207003](#)].
- [23] M. Porrati, *Higgs phenomenon for the graviton in AdS space*, *Mod. Phys. Lett.* **A 18** (2003) 1793 [[hep-th/0306253](#)].
- [24] O. Aharony, O. DeWolfe, D.Z. Freedman and A. Karch, *Defect conformal field theory and locally localized gravity*, *JHEP* **07** (2003) 030 [[hep-th/0303249](#)].
- [25] R. Gregory, S.F. Ross and R. Zegers, *Classical and quantum gravity of brane black holes*, *JHEP* **09** (2008) 029 [[arXiv:0802.2037](#)].
- [26] R. Gregory, *Braneworld black holes*, [arXiv:0804.2595](#).
- [27] T. Hirayama and G. Kang, *Stable black strings in anti-de Sitter space*, *Phys. Rev.* **D 64** (2001) 064010 [[hep-th/0104213](#)].
- [28] A. Chamblin and A. Karch, *Hawking and Page on the brane*, *Phys. Rev.* **D 72** (2005) 066011 [[hep-th/0412017](#)].
- [29] L. Grisa and O. Pujolàs, *Dressed Domain Walls and Holography*, *JHEP* **06** (2008) 059 [[arXiv:0712.2786](#)].
- [30] S. Nojiri and S.D. Odintsov, *Brane world inflation induced by quantum effects*, *Phys. Lett.* **B 484** (2000) 119 [[hep-th/0004097](#)].
- [31] S. Nojiri and S.D. Odintsov, *AdS/CFT correspondence, conformal anomaly and quantum corrected entropy bounds*, *Int. J. Mod. Phys.* **A 16** (2001) 3273 [[hep-th/0011115](#)].
- [32] T. Shiromizu and D. Ida, *Anti-de Sitter no hair, AdS/CFT and the brane-world*, *Phys. Rev.* **D 64** (2001) 044015 [[hep-th/0102035](#)].
- [33] T. Shiromizu, T. Torii and D. Ida, *Brane-world and holography*, *JHEP* **03** (2002) 007 [[hep-th/0105256](#)].
- [34] J. Garriga and T. Tanaka, *Gravity in the brane-world*, *Phys. Rev. Lett.* **84** (2000) 2778 [[hep-th/9911055](#)].
- [35] M.J. Duff and J.T. Liu, *Complementarity of the Maldacena and Randall-Sundrum pictures*, *Class. and Quant. Grav.* **18** (2001) 3207 [*Phys. Rev. Lett.* **85** (2000) 2025] [[hep-th/0003237](#)].
- [36] I. Giannakis, J.T. Liu and H.-c. Ren, *Linearized gravity in the Karch-Randall braneworld*, *Nucl. Phys.* **B 654** (2003) 197 [[hep-th/0211196](#)].
- [37] S.W. Hawking, T. Hertog and H.S. Reall, *Trace anomaly driven inflation*, *Phys. Rev.* **D 63** (2001) 083504 [[hep-th/0010232](#)].

- [38] T. Tanaka, *AdS/CFT correspondence in a Friedmann-Lemaitre-Robertson-Walker brane*, [gr-qc/0402068](#).
- [39] R. Casadio, *Holography and trace anomaly: what is the fate of (brane-world) black holes?*, *Phys. Rev. D* **69** (2004) 084025 [[hep-th/0302171](#)].
- [40] R. Emparan, G.T. Horowitz and R.C. Myers, *Exact description of black holes on branes*, *JHEP* **01** (2000) 007 [[hep-th/9911043](#)].
- [41] R. Emparan, G.T. Horowitz and R.C. Myers, *Exact description of black holes on branes. II: comparison with BTZ black holes and black strings*, *JHEP* **01** (2000) 021 [[hep-th/9912135](#)].
- [42] M. Anber and L. Sorbo, *Two gravitational shock waves on the AdS₃ brane*, *JHEP* **10** (2007) 072 [[arXiv:0706.1560](#)].
- [43] M. Anber and L. Sorbo, *New exact solutions on the Randall-Sundrum 2-brane: lumps of dark radiation and accelerated black holes*, *JHEP* **07** (2008) 098 [[arXiv:0803.2242](#)].
- [44] N. Kaloper and L. Sorbo, *Locally localized gravity: the inside story*, *JHEP* **08** (2005) 070 [[hep-th/0507191](#)].
- [45] H. Narnhofer, I. Peter and W.E. Thirring, *How hot is the de Sitter space?*, *Int. J. Mod. Phys. B* **10** (1996) 1507.
- [46] S. Deser and O. Levin, *Accelerated detectors and temperature in (anti) de Sitter spaces*, *Class. and Quant. Grav.* **14** (1997) L163 [[gr-qc/9706018](#)].
- [47] J.G. Russo and P.K. Townsend, *Accelerating Branes and Brane Temperature*, *Class. and Quant. Grav.* **25** (2008) 175017 [[arXiv:0805.3488](#)].
- [48] P. Candelas and D. Deutsch, *On the vacuum stress induced by uniform acceleration or supporting the ether*, *Proc. Roy. Soc. Lond. A* **354** (1977) 79.
- [49] V.P. Frolov and E.M. Serebryanyi, *Quantum effects in systems with accelerated mirrors*, *J. Phys. A* **12** (1979) 2415.
- [50] R.D. Carlitz and R.S. Willey, *Reflections on moving mirrors*, *Phys. Rev. D* **36** (1987) 2327.
- [51] O. Pujolàs and T. Tanaka, *Massless scalar fields and infrared divergences in the inflationary brane world*, *JCAP* **12** (2004) 009 [[gr-qc/0407085](#)].
- [52] J.P. Norman, *Casimir effect between anti-de Sitter braneworlds*, *Phys. Rev. D* **69** (2004) 125015 [[hep-th/0403298](#)].
- [53] T.M. Helliwell and D.A. Konkowski, *Vacuum fluctuations outside cosmic strings*, *Phys. Rev. D* **34** (1986) 1918.
- [54] V.P. Frolov and E.M. Serebryanyi, *Vacuum polarization in the gravitational field of a cosmic string*, *Phys. Rev. D* **35** (1987) 3779.
- [55] J.S. Dowker, *Casimir effect around a cone*, *Phys. Rev. D* **36** (1987) 3095.
- [56] J.S. Dowker, *Vacuum averages for arbitrary spin around a cosmic string*, *Phys. Rev. D* **36** (1987) 3742.
- [57] R. Emparan, *AdS/CFT duals of topological black holes and the entropy of zero-energy states*, *JHEP* **06** (1999) 036 [[hep-th/9906040](#)].
- [58] G. Dvali, *Black holes and large-N species solution to the hierarchy problem*, [arXiv:0706.2050](#).

- [59] G. Dvali and M. Redi, *Black Hole Bound on the Number of Species and Quantum Gravity at LHC*, *Phys. Rev. D* **77** (2008) 045027 [arXiv:0710.4344].
- [60] G. Dvali, G. Gabadadze, O. Pujolàs and R. Rahman, *Domain walls as probes of gravity*, *Phys. Rev. D* **75** (2007) 124013 [hep-th/0612016].
- [61] G.R. Dvali, G. Gabadadze and M. Porrati, *4D gravity on a brane in 5D Minkowski space*, *Phys. Lett. B* **485** (2000) 208 [hep-th/0005016].
- [62] J. Garriga, O. Pujolàs and T. Tanaka, *Radion effective potential in the Brane-World*, *Nucl. Phys. B* **605** (2001) 192 [hep-th/0004109].
- [63] S.S. Gubser, I.R. Klebanov and A.W. Peet, *Entropy and temperature of black 3-branes*, *Phys. Rev. D* **54** (1996) 3915 [hep-th/9602135].
- [64] V. Balasubramanian and P. Kraus, *A stress tensor for anti-de Sitter gravity*, *Commun. Math. Phys.* **208** (1999) 413 [hep-th/9902121].
- [65] V. Balasubramanian and S.F. Ross, *The dual of nothing*, *Phys. Rev. D* **66** (2002) 086002 [hep-th/0205290].
- [66] R. Gregory and A. Padilla, *Nested braneworlds and strong brane gravity*, *Phys. Rev. D* **65** (2002) 084013 [hep-th/0104262].
- [67] A. Vilenkin and E. Shellard, *Cosmic strings and other topological defects*, Cambridge University Press, Cambridge U.K. (1994).